X-612-69-446

PREPRINT

NASA TM X- 63724

A METHOD USED FOR THE DETERMINATION OF THE EXPLORER XXVI SPIN AXIS POSITION

P. A. BRACKEN
L. R. DAVIS
R. W. JANETZKE

OCTOBER 1969

GODDARD SPACE FLIGHT CENTER
GREENBELT, MARYLAND

X-612-69-446
PREPRINT
NASA TM X- 63724

A METHOD USED FOR THE DETERMINATION OF THE EXPLORER XXVI SPIN AXIS POSITION

P. A. BRACKEN
L. R. DAVIS
R. W. JANETZKE

OCTOBER 1969

GSFC
GODDARD SPACE FLIGHT CENTER
GREENBELT, MARYLAND

X-612-69-446

A METHOD USED FOR THE DETERMINATION OF THE EXPLORER XXVI SPIN AXIS POSITION

P. A. Bracken
L. R. Davis
R. W. Janetzke

October 1969

GODDARD SPACE FLIGHT CENTER
Greenbelt, Maryland

A METHOD USED FOR THE DETERMINATION OF THE EXPLORER XXVI SPIN AXIS POSITION

P. A. Bracken
L. R. Davis
R. W. Janetzke

ABSTRACT

Two series of least squares fits were performed to determine the Explorer XXVI spin axis position in celestial coordinates throughout orbits 1 to 533. The data input to the calculations consisted of the sun's position, Jensen-Cain magnetic field positions, the sun-spin axis angle, values of the magnetic field-spin axis angle and values of the angle between the spin-sun and the spin-field planes. The latter three angles were derived from the on-board Solar Aspect detector and from the roll modulated output curve of the Ion and Electron particle experiment.

The results of the fits are presented as a table listing a spin axis right ascension-declination pair along with the uncertainties in these angles for each orbit through orbit 533.

ACKNOWLEDGMENTS

The authors wish to thank Dr. W. E. Daniels for the use of his general least squares fitting program GLSWS.

The authors also thank Mr. H. M. Caulk for the use of his spherical triangle solver CAAAB and for the program HELOS which supplied the sun's position in celestial coordinates. Special thanks must also go to Mr. Caulk for the valuable assistance he rendered in checking parts of the programs and in helping to debug some early magnetic tape and I/O problems that were encountered.

CONTENTS

ILLUSTRATIONS

TABLES

A METHOD USED FOR THE DETERMINATION OF THE EXPLORER XXVI SPIN AXIS POSITION

INTRODUCTION

This report describes a method used to find the Explorer XXVI spin axis position in celestial coordinates as a function of time through orbit 533.

The determination was based on knowing the sun's position, the magnetic field position (Jensen-Cain field, Reference [4]) and values of the angles:

1. λ-the angle between the spin axis and sun positions,

2. α-the angle between the spin axis and magnetic field positions, and

3. ψ-the angle between the spin axis-sun and the spin axis-field planes measured in the direction of spacecraft rotation.

Data values for the angle λ were gotten directly from the Explorer XXVI Digital Solar Aspect Sensor (as described in Reference [1]). Data values of the angles α and ψ were determined from the roll modulated output curve of the Explorer XXVI Ion-Electron particle experiment (as described in Reference [8]).

A non-linear least squares fitting program GLSWS was used in two separate series of fits to obtain the final spin axis coordinates. During the first series of fits, the sun and magnetic field positions along with values of λ, α and ψ from one orbit were used to obtain a determination of the spin axis position. Because of the data selection criteria used in the first series of fits, from four to twenty separate determinations were possible for each orbit through orbit 540.

A second series of GLSWS fits were performed fitting parabolas to the results of the first series of GLSWS determinations versus orbit number. The parabola fits were performed on fifteen orbit batches. The final spin axis coordinates of the mid orbit of a fifteen orbit batch were taken as the value of the fitted parabola at that mid orbit. The fifteen orbit batches were slid up one orbit at a time allowing final spin axis determinations for orbits 7 through 533.

CHAPTER I

PRELIMINARY CONCEPTS

A. THE BASIC PROBLEM

The objective of the study described in this report was to determine the Explorer XXVI (EPE-D) spin axis orientation as a function of time in inertial coordinates. The determination was performed on orbits 1 through 533, a period during which Explorer XXVI was spin stabilized. *

The data used in the determination consisted of:

1. measurements of the spin axis-sun angle, λ, provided by the on-board solar aspect sensor,

2. values of the angle (ψ) from the sun-spin axis plane to the magnetic field-spin axis plane measured in the direction of spacecraft rotation,

3. values of the angle (α) between the magnetic field and spin axis positions, and

4. the statistical uncertainties σ_λ, σ_ψ and σ_α in λ, ψ and α.

The angles λ, α and ψ are shown in Figure 1 for one possible sun, magnetic field, spin axis orientation.

The magnetic field position in celestial coordinates was that given by the Jensen and Cain Magnetic Field Coefficients for 1960 (see Reference [4]).

The sun's position in celestial coordinates was derived by using the computer program HELOS as described in Reference [6].

Values of the α and ψ angles were derived from solar aspect data and from the Ion and Electron detector's roll modulated output curve. For a description of the I&E detector see Reference [8].

As is illustrated in Figure 2, λ and α fix the spin axis position to the intersections of circles of constant α and of constant λ on the celestial sphere. If in

*Explorer XXVI was launched on December 21, 1964. Orbits 1-533 cover the approximate time period from day 356.3927 (December 21, 1964) to day 524.9595 (June 7, 1965).

addition, the angle ψ is known then ambiguity is eliminated and the true spin axis position (i.e. either SA_1 or SA_2 in Figure 2) can be determined. (The direction of rotation of the spacecraft was known.)

In general, knowledge of any two of the angles λ, α and ψ will yield two possible spin axis positions and knowledge of all three of the angles will resolve the ambiguity. In practice, there are cases when knowledge of only two of λ, α or ψ is sufficient for a spin axis determination because:

1. the spin axis location moves slowly with time and its position is known well enough to resolve ambiguity, and

2. a number of α and ψ values can be used over periods of up to one hour during which time the field direction will change significantly thus helping to resolve the spin axis ambiguity.

B. RELATIONSHIP OF ψ AND α TO THE I&E DETECTOR OUTPUT CURVE

Charged particles having small pitch angles* are lost into the atmosphere. For this reason, the I&E detector will measure a minimum in particle intensity when looking along a magnetic field line. Similarly, a maximum in particle intensity occurs when the I&E detector measures particles having 90° pitch angles—that is, when the I&E detector is pointing in a direction 90° away from the field line. This response was found to be empirically true for the I&E detector at selected times and was assumed to be true for all times.

On Explorer XXVI, the I&E detector was mounted at a 45° angle to the spacecraft spin axis so that a cone of half angle 45° was swept out about the spin axis by the I&E detector during each roll. By making use of the solar aspect data provided on Explorer XXVI, the output of the I&E detector can be plotted against the fraction of a roll after see sun at which each I&E measurement was taken.

A direct reading from such a roll modulated output curve of the abscissa corresponding to a minimum in particle intensity will yield either ψ or $\psi \pm 180°$. Figure 3 illustrates the point for one possible roll modulation pattern. In Figure 3, the abscissa x_1 represents the fraction of a roll after see sun at which the I&E detector was looking in either the plus field or the minus field directions.

*The pitch angle is the angle between the particle velocity vector and the magnetic field vector at a point in space.

(Similarly for the abscissa x_2). Together x_1 and x_2 correspond to one pair of values from the set $\{\psi, \psi + 180°, \psi - 180°\}$.

The relationship of α to the I&E roll modulation curve can be seen by examining Figure 4. The Law of Cosines applied to the spherical triangle in Figure 4 with arcs α, 90° and 45° yields:

$$\cos 90° = \cos 45° \cdot \cos \alpha + \sin 45° \cdot \sin \alpha \cdot \cos (180° - f/2) \quad (1.1)$$

where f is the fraction of a roll between maximum particle intensity readings by the I&E detector during one roll.

Solving Equation 1.1 for α gives

$$\alpha = 90° - \arctan \left(\cos (f/2)\right) . \quad (1.2)$$

Thus it is seen that α is a function of the fraction of a roll between maximum particle intensities as measured by the I&E detector.

As with ψ, the determination of α from the I&E output curve can yield either α or $180° - \alpha$. Thus the α, ψ data used in the spin axis determinations are ambiguous in that it is not known whether they are measured with respect to the positive or negative field direction at any given time.

Examples of possible I&E detector output curves are given in Figures 5 and 6.

Further information on the actual method used to calculate α and ψ from the I&E detector data is given in Reference [3]. Suffice it to say that in practice ψ can always be found from the I&E data but that α cannot be calculated outside the range $60° < \alpha < 120°$. When α is less than 60° or greater than 120°, maximum intensity occurrences are either too flat or otherwise too ill defined on the I&E roll modulation curve to be used in a determination of α.

C. DETERMINATION OF THE SPIN AXIS-SUN ANGLE

The solar aspect sensor on board Explorer XXVI provided digitized measurements of the sun-spin axis angle, λ. The solar aspect detector, with a fan field of vision 180 degrees in length, was mounted so that the fan swept out the entire sky as the satellite rotated.

The nominal uncertainty in the sun-spin angle measurements was ±1.5° since the solar aspect detector sampled the 180° fan in 63 approximately equal intervals. However when the λ-reading changes from one of the 63 sectors to another, the angle is known more accurately—to approximately ±0.3 degrees. Also when the motion of the spin axis is regular with respect to the sun, the angle λ may be interpolated to this higher accuracy.

For further information on the solar aspect detector see References [1] and [2].

CHAPTER II

METHOD FOR SPIN AXIS DETERMINATION

A. THE MATHEMATICAL PROCEDURE FOLLOWED

Denote the right ascension and declination of the sun, magnetic field and spin axis by SRA, SDC, FRA, FDC, ARA and ADC respectively. Using this notation, the angles λ, α and ψ can be written as

$$\begin{aligned} \lambda &= f(\text{ARA, ADC, SRA, SDC}) \\ \alpha &= g(\text{ARA, ADC, SRA, SDC, FRA, FDC}) \\ \psi &= h(\text{ARA, ADC, SRA, SDC, FRA, FDC}) \end{aligned} \tag{2.1}$$

where f, g and h are unknown functions.

For a given time period the following data are known:

a. the sun-spin axis angle Λ

b. the celestial coordinates SRA, SDC of the sun

c. n values of ψ as Ψ_i and the associated field coordinates FRA_i, FDC_i.

d. m values of α as A_j and the associated field coordinates values FRA_j, FDC_j, and

e. the statistical uncertainties σ_Λ, $\{\sigma_{\Psi_i}\}_{i=1}^{n}$ and $\{\sigma_{A_j}\}_{j=1}^{m}$ for the angles in (a), (c) and (d) respectively.

The problem was to find those values of the spin axis coordinates ARA and ADC which when used in Equations 2.1 along with the proper field and sun coordinates would yield a minimum value for the expression:

$$\chi^2 = \left(\frac{\Lambda - \lambda}{\sigma_\Lambda}\right)^2 + \sum_{i=1}^{n}\left(\frac{\Psi_i - \psi_i}{\sigma_{\Psi_i}}\right)^2 + \sum_{j=1}^{m}\left(\frac{A_j - \alpha_j}{\sigma_{A_j}}\right)^2 \tag{2.2}$$

where λ, ψ_i and α_j are the calculated values yielded from Equations 2.1 and Λ, Ψ_i, A_j are the measured data values.

Given the data as listed in (a)-(e) above, a modified version of W. E. Daniels' General Least Squares (GLSWS) program was used to solve for the spin axis coordinates during given time periods. A description of GLSWS is given in Reference [7].

For ease in using GLSWS, Equations 2.1 were rewritten in one equation as

$$y = F(ARA, ADC, SRA, SDC, FRA, FDC, I) \qquad (2.3)$$

where the independent variable I is 1, 2 or 3 for the function F to yield values of λ, α or ψ respectively.

In conjunction with the notation used in Reference [7], Equation 2.3 was written as

$$y = F(P1, P2, x_1, x_2, x_3, x_4, x_5) \qquad (2.4)$$

where P1 and P2 are the spin axis right ascension and declination and x_1 through x_5 are SRA, SDC, FRA, FDC and I respectively as in Equation 2.3.

The program GLSWS uses an iterative algorithm to accomplish the required fit. To initialize the algorithm, it was required that the following values be fed to GLSWS:

a. guess values of ARA and ADC as $P1_0$ and $P2_0$

b. k data values Y_i and $(X_{1i}, \cdots, X_{5i})$

c. k calculated values y_i (derived from Equation 2.4) using the values $(X_{1i}, \cdots, X_{5i})$ and $P1_0, P2_0$

d. the partial derivatives

$$\left(\frac{\partial F}{\partial P1}\right)_{P1_0, P2_0, X_{1i}, \cdots, X_{5i}}$$

$$\left(\frac{\partial F}{\partial P2}\right)_{P1_0, P2_0, X_{1i}, \cdots, X_{5i}} \tag{2.5}$$

for $i = 1, \cdots, k$.

In return, GLSWS yielded new values of P1 and P2 which minimized the expression

$$RMS = \sqrt{\frac{\sum_{i=1}^{k} (y_i - Y_i)^2}{k - 2}} \, . \tag{2.6}$$

Since the form of the function F in Equation 2.4 was quite long and complicated, a practical method of calculating the values in (c) and (e) above was evolved. This method consisted in utilizing the known celestial coordinates of the sun and field positions together with the guess coordinates of the spin axis position to obtain spherical triangle solutions yielding calculated values y_i for λ, α and ψ. For example, in Figure 7 the codeclination of the sun and spin axis along with the difference in their right ascensions provides enough information to solve the given spherical triangle for λ. Similarly, spherical triangle solutions may be obtained for α and ψ. In practice, the program CAAAB as described in Reference [5] was used to solve the required spherical triangles. Using the above procedure, spherical triangle solutions were found for the k required calculated values:

$$y_i = F(P1_0, P2_0, X_{1i}, \cdots, X_{5i}) \, . \tag{2.7}$$

In addition, the guess values $P1_0$ and $P2_0$ were incremented by an amount Δ* and these incremented values were used in spherical triangle solutions to obtain the calculated values:

$$y_i' = F(P1_0 + \Delta, P2_0, X_{1i}, \cdots, X_{5i})$$

$$y_i'' = F(P1_0, P2_0 + \Delta, X_{1i}, \cdots, X_{5i}) \, . \tag{2.8}$$

*In our calculations Δ was taken to be one degree.

Finally the required partial derivatives were calculated from:

$$\left(\frac{\partial F}{\partial P1}\right)_{P1_0, P2_0, X_{1i}, \cdots, X_{5i}} = \frac{y_i' - y_i}{\Delta}$$

$$\left(\frac{\partial F}{\partial P2}\right)_{P1_0, P2_0, X_{1i}, \cdots, X_{5i}} = \frac{y_i'' - y_i}{\Delta} \quad . \tag{2.9}$$

At the beginning of the $n+1^{st}$ iteration, the values y_i and the required partial derivatives were calculated from Equations 2.7, 2.8 and 2.9 using the values $P1_n$ and $P2_n$ of the spin axis coordinates returned by GLSWS at the end of the n^{th} iteration. This procedure was allowed to continue until successive iterates were close enough (difference $<10^{-2}$ degrees) or until the number of iterations exceeded a specified value.

B. THE METHOD AND INPUT DATA USED

In practice, the mathematical procedure and the data input to GLSWS were modified slightly to force GLSWS to perform a weighted least squares fit utilizing the known uncertainties σ_λ, σ_α and σ_ψ.

To accomplish the weighted fit, the basic equation (Equation 2.7) was utilized to obtain a new set of calculated values as:

$$z_i = \frac{y_i - Y_i}{\sigma_{Y_i}} \tag{2.10}$$

where Y_i, σ_{Y_i} are the measured data values and their uncertainties and where y_i is given by Equation 2.7 for $i = 1, \ldots, k$.

Redefining the basic expression as in Equation 2.10 caused GLSWS to perform the weighted fit while minimizing the expression:

$$\text{RMS} = \sqrt{\frac{(z_i - 0.0)^2}{k-2}}$$

or

$$\text{RMS} = \sqrt{\frac{\left(\frac{y_i - Y_i}{\sigma_{Y_i}}\right)^2}{k-2}} \quad . \tag{2.11}$$

Also the partial derivatives supplied to GLSWS became:

$$\left(\frac{\partial z_i}{\partial P1}\right)_{P1_n, P2_n} = \frac{1}{\sigma_{Y_i}} \cdot \left(\frac{\partial F}{\partial P1}\right)_{P1_n, P2_n, X_{1i}, \cdots, X_{5i}} \tag{2.12}$$

and

$$\left(\frac{\partial z_i}{\partial P2}\right)_{P1_n, P2_n} = \frac{1}{\sigma_{Y_i}} \cdot \left(\frac{\partial F}{\partial P2}\right)_{P1_n, P2_n, X_{1i}, \cdots, X_{5i}} \tag{2.13}$$

where $i = 1, \cdots, k$.

In summary, to initiate a fit GLSWS was supplied with:

a. k values of Y_i, σ_{Y_i} and $(X_{1i}, \cdots, X_{5i})$

b. guess values $P1_0$ and $P2_0$ for P1 and P2

c. k values of z_i calculated from Equation 2.10 and

d. k partial derivatives $\partial z_i/\partial P1$, $\partial z_i/\partial P2$ as calculated from Equations 2.12 and 2.13 using $(P1_0, P2_0)$ for $(P1_n, P2_n)$.

The data supplied to GLSWS for a spin axis determination were selected according to the following criteria:

1. the data for each fit had to be from the same orbit

2. the data for each fit had to extend over a time period of no longer than one hour

3. the data used for a fit had to extend over an interval of no larger than .5 earth radii in L value (ex. data from L = 3.0 to L = 3.5) and

4. the total number of points used for a fit had to be at least four but less than ninety-seven.

For any given fit during which k data values were supplied to GLSWS, k was comprised of one value of λ, n values of α and $k - n - 1$ values of ψ where n varied from 0 to $(k - 1)/2$.

The uncertainties σ_α and σ_ψ in α and ψ were fixed at three degrees and two degrees respectively. The data values for α and ψ were read in from magnetic tapes whose format is described in Reference [3].

The data values used for λ and σ_λ are tabulated in Table 1. The gaps in this table were filled in by linear interpolation.

CHAPTER III

CONCLUSION

A. PRESENTATION AND DISCUSSION OF THE RESULTS DERIVED

As a result of the criteria applied during input data selection, there were as many as twenty separate spin axis determinations made by GLSWS for each orbit in the range from orbit 1 to orbit 540.

A plot of the twenty or so spin axis determinations for each orbit from the first round of GLSWS fittings showed considerable scatter in these results. To eliminate this scatter and to achieve the most reliable final result, an additional fit was performed on the spin axis coordinates determined from the first round of GLSWS fits. In this second GLSWS fit, parabolas were fitted to the spin axis coordinates from the first GLSWS determinations on fifteen orbit batches. The coordinates yielded from the fitted parabolas for the mid orbit of each fifteen orbit batch were taken as the final spin axis position for that orbit. Also the fifteen orbit batches were slid up one orbit at a time so that the coordinates for orbit n were derived from a fit to the GLSWS determinations for orbits n - 7 to n + 7.

In addition, only those original determinations (of the twenty or so possibilities) which resulted from fits having at least ninety percent as many α's as ψ's and which arose from data having L values between 1.5 and 4.5 were used in the final parabola fits. Consequently, only from three to ten of the twenty possible original determinations per orbit were used as input data for the fifteen orbit parabola fits.

The results of the final parabola fits are listed in Table 2. Columns three through eight of Table 2 are expressed in degrees. Column two lists orbit start times in day plus fraction of the day where the following conventions hold:

1. launch occurred on December 21, 1964 (day 356. of 1964)

2. day 367. corresponds to January 1, 1965 (since 1964 was a leap year)

3. day 524. corresponds to June 7, 1965.

Columns three and four of Table 2 list the final values of the spin axis right ascension and declination respectively. Columns seven and eight are the final values of the parabola fit RMS yielded by GLSWS (as expressed in Equation 2.6). Columns five and six are the uncertainties in columns three and four respectively

and were determined from:

$$\sigma_{RA} = RMS_{RA} \cdot \sqrt{D_{11}}$$

$$\sigma_{DEC} = RMS_{DEC} \cdot \sqrt{D_{11}'} \qquad (3.1)$$

D_{11} and D_{11}' are the first elements of the inverse coefficient matrices from the final parabola fits in GLSWS.

The coordinates listed in Table 2 for orbits one through seven are "eyeball" extrapolations obtained from a plot of the remainder of the table from orbit eight on. Consequently, the uncertainty and RMS values in columns five through eight for the first seven orbits are listed as "999.".

A plot of the results listed in Table 2 appears in Figure 8.

B. LIMITATIONS OF THE METHOD USED

In some orientations of the spin axis, sun, field positions one of the spin axis coordinates can be heavily dependent on one of λ, α or ψ. Thus for a good spin axis determination in such cases, values of that angle must be present in the input data fed to GLSWS during the first round of fits. For example, from orbit 400 on the Explorer XXVI spin axis declination was ill determined when only values of λ and ψ were used for a determination. For this reason, only those spin axis determinations calculated for time periods with λ, α and ψ values present in the input data were used to obtain the final results. For the calculations from orbit 400 on, best determinations were made when there were almost as many α's as ψ's present in a block of data fed to GLSWS during the first round fits.

It was also found that data associated with L values greater than 4.5 sometimes yielded erroneous spin axis determinations. For this reason the input data used were restricted to L shells in the range $1.5 \leq L \leq 4.5$.

The erroneous spin axis determinations probably resulted for one or more of the following reasons:

1. at certain times the effects of magnetic disturbances were still significant down to L shells of L = 4.5, or

2. flat pitch angle distributions were encountered yielding inaccurate determinations of α and ψ from the I&E detector output, or

3. count rates went down while statistical fluctuations became larger.

REFERENCES

1. Albus, J. S., A digital solar aspect sensor, NASA TN D-1062, National Aeronautics and Space Administration, Washington, D. C., Sept. 1961.

2. Albus, J. S. and Schaefer, D. H., Satellite attitude determination: digital sensing and on-board processing, IEEE Transactions on Space Electronics and Telemetry, Sept. 1963, Vol. SET-9, 71-77.

3. Bracken, P. A. and Davis, L. R., User's manual for the S3XPSA program, obtainable from the authors, NASA/GSFC, Greenbelt, Md.

4. Cain, J. C., et al., Computation of the main geomagnetic field from spherical harmonic expansions, NASA X-611-64-316, NASA Goddard Space Flight Center, Greenbelt, Md., Oct. 1964.

5. Caulk, H. M., CAAAB program documentation, obtainable from the author, NASA/GSFC, Greenbelt, Md.

6. Caulk, H. M., HELOS program documentation, obtainable from the author, NASA/GSFC, Greenbelt, Md.

7. Daniels, W. E., GLSWS—General least squares with statistics, Tech. Report No. 579, Dept. of Physics, Univ. of Maryland, College Park, Md., July 1966.

8. Davis, L. R. and Williamson, J. M., Outer Zone Protons, Proc. NATO Advanced Study Institute, Bergen, Norway, August 1965, Radiation Trapped in the Earth's Magnetic Field, Edited by B. M. McCormac, D. Reidel Publishing Co., Dordrecht, Holland, 215, 1966.

APPENDIX A

NOTATION

Λ, λ – the spin axis-sun angle.

α, A – the spin axis-magnetic field angle.

ψ, Ψ – the angle between the spin-sun and the spin-field planes measured in the direction of spacecraft rotation.

σ_λ, σ_Λ – the statistical uncertainty in λ, Λ.

σ_α, σ_A – the statistical uncertainty in α, A.

σ_ψ, σ_Ψ – the statistical uncertainty in ψ, Ψ.

ARA – spin axis right ascension.

ADC – spin axis declination.

SRA – sun right ascension.

SDC – sun declination.

FRA – magnetic field right ascension.

FDC – magnetic field declination.

y_i – a calculated value of λ, α or ψ.

Y_i – a measured value of λ, α or ψ.

APPENDIX B

TABLES

Table 1

Values of the Spin Axis-Sun Angle

Time (day + fraction)	λ (degrees)	σ_λ (degrees)
356.00	46.1	±1.0
377.00	46.5	1.0
383.65	48.9	0.3
389.74	50.4	0.3
398.60	55.3	0.3
401.84	57.4	0.3
408.15	60.2	0.3
412.35	62.6	0.3
417.73	66.1	0.3
421.44	69.3	0.3
427.15	73.1	0.3
431.27	74.8	0.3
437.25	78.9	0.3
439.61	81.3	0.3
445.88	84.6	0.3
449.57	86.8	0.3
454.62	90.7	0.3
457.45	92.6	0.3
464.09	96.5	0.3
468.38	98.4	0.3
475.90	101.3	0.3
480.33	104.6	0.3
488.27	108.0	0.3
493.52	110.3	0.3
500.17	113.6	0.3
513.70	116.7	0.3
524.00	118.0	1.2
534.43	116.7	0.3
557.03	115.2	1.6
579.63	116.4	0.3
595.20	118.8	2.0

Table 2

Explorer XXVI Spin Axis Coordinates to Orbit 533

ORB.	START TIME	RT. ASCEN.	DEC.	SIG. R.A.	SIG. DEC.	RMS R.A.	RMS DEC.
1.	356.3829	272.8	21.5	999.	999.	999.	999.
2.	356.6996	272.8	21.5	999.	999.	999.	999.
3.	357.0164	272.8	21.5	999.	999.	999.	999.
4.	357.3331	272.8	21.4	999.	999.	999.	999.
5.	357.6499	272.9	21.4	999.	999.	999.	999.
6.	357.9666	272.9	21.4	999.	999.	999.	999.
7.	358.2833	272.9	21.4	999.	999.	999.	999.
8.	358.6001	272.9	21.2	0.25	0.31	1.13	1.49
9.	358.9168	273.0	21.4	0.23	0.34	1.14	1.65
10.	359.2335	273.1	21.4	0.22	0.35	1.11	1.73
11.	359.5503	273.2	21.2	0.22	0.35	1.09	1.72
12.	359.8670	273.1	21.4	0.23	0.38	1.14	1.87
13.	360.1837	273.0	21.3	0.23	0.34	1.14	1.70
14.	360.5004	273.0	21.2	0.23	0.34	1.14	1.69
15.	360.8171	272.9	20.9	0.22	0.35	1.06	1.70
16.	361.1339	272.9	20.8	0.22	0.35	1.11	1.68
17.	361.4507	272.9	20.9	0.23	0.36	1.13	1.72
18.	361.7674	273.0	20.7	0.22	0.36	1.07	1.69
19.	362.0841	273.0	20.6	0.24	0.37	1.12	1.70
20.	362.4008	273.1	20.6	0.24	0.37	1.15	1.72
21.	362.7176	273.1	20.5	0.23	0.41	1.09	1.94
22.	363.0342	273.1	20.5	0.25	0.39	1.18	1.77
23.	363.3510	273.2	20.7	0.25	0.38	1.16	1.75
24.	363.6677	273.2	20.6	0.24	0.35	1.10	1.62
25.	363.9844	273.0	20.9	0.30	0.47	1.36	2.13
26.	364.3011	273.0	20.8	0.26	0.47	1.21	2.16
27.	364.6179	273.0	20.5	0.25	0.39	1.16	1.81
28.	364.9346	272.9	20.5	0.27	0.39	1.23	1.79
29.	365.2512	273.0	20.4	0.26	0.39	1.21	1.80
30.	365.5680	273.1	20.3	0.27	0.33	1.22	1.47

Table 2 (continued)

ORB.	START TIME	RT. ASCEN.	DEC.	SIG. R.A.	SIG. DEC.	RMS R.A.	RMS DEC.
31.	365.8847	273.1	20.6	0.32	0.44	1.47	1.95
32.	366.2014	273.2	20.2	0.32	0.42	1.46	1.89
33.	366.5181	273.3	20.0	0.33	0.44	1.48	1.95
34.	366.8349	273.3	20.0	0.33	0.50	1.47	2.25
35.	367.1516	273.2	19.8	0.32	0.44	1.46	1.97
36.	367.4683	273.2	19.8	0.34	0.50	1.51	2.22
37.	367.7850	273.0	19.9	0.34	0.50	1.49	2.22
38.	368.1017	272.9	19.9	0.34	0.49	1.48	2.17
39.	368.4184	272.7	20.0	0.35	0.52	1.52	2.21
40.	368.7351	272.8	19.6	0.31	0.35	1.29	1.42
41.	369.0518	272.7	19.7	0.31	0.33	1.29	1.38
42.	369.3685	272.7	19.8	0.32	0.34	1.32	1.39
43.	369.6852	272.7	19.8	0.29	0.35	1.21	1.45
44.	370.0019	272.6	20.0	0.31	0.34	1.28	1.39
45.	370.3187	272.6	20.1	0.31	0.38	1.26	1.56
46.	370.6353	272.7	19.9	0.24	0.28	1.02	1.18
47.	370.9521	272.7	20.0	0.26	0.28	1.09	1.18
48.	371.2687	272.7	20.0	0.25	0.28	1.06	1.19
49.	371.5855	272.7	19.9	0.24	0.24	1.02	1.03
50.	371.9021	272.9	20.2	0.25	0.29	1.07	1.22
51.	372.2189	272.8	20.1	0.24	0.27	1.04	1.21
52.	372.5356	272.8	20.1	0.24	0.28	1.04	1.23
53.	372.8523	272.7	19.9	0.24	0.30	1.07	1.32
54.	373.1690	272.6	19.8	0.23	0.29	1.02	1.29
55.	373.4857	272.6	19.7	0.24	0.30	1.05	1.33
56.	373.8024	272.5	19.6	0.25	0.31	1.06	1.32
57.	374.1191	272.4	19.3	0.25	0.29	1.08	1.25
58.	374.4358	272.4	19.3	0.27	0.31	1.11	1.28
59.	374.7525	272.5	19.1	0.25	0.30	1.04	1.26
60.	375.0692	272.5	19.1	0.26	0.30	1.06	1.25

Table 2 (continued)

ORB.	START TIME	RT. ASCEN.	DEC.	SIG. R.A.	SIG. DEC.	RMS R.A.	RMS DEC.
61.	375.3859	272.6	19.2	0.27	0.32	1.09	1.29
62.	375.7026	272.7	19.2	0.24	0.32	0.99	1.31
63.	376.0192	272.8	19.4	0.26	0.31	1.07	1.26
64.	376.3360	273.0	19.6	0.26	0.30	1.06	1.19
65.	376.6526	273.0	19.6	0.25	0.26	1.01	1.06
66.	376.9694	272.9	19.6	0.25	0.26	1.01	1.05
67.	377.2860	273.0	19.6	0.24	0.25	0.98	1.03
68.	377.6027	272.9	19.5	0.25	0.24	0.99	0.97
69.	377.9194	272.9	19.5	0.28	0.24	1.08	0.94
70.	378.2361	272.9	19.5	0.27	0.23	1.05	0.93
71.	378.5528	272.9	19.4	0.26	0.23	1.01	0.89
72.	378.8695	272.9	19.3	0.24	0.21	0.94	0.83
73.	379.1862	272.9	19.4	0.23	0.20	0.92	0.81
74.	379.5028	272.8	19.5	0.24	0.20	0.95	0.78
75.	379.8195	272.8	19.5	0.23	0.18	0.93	0.75
76.	380.1362	272.8	19.5	0.21	0.17	0.89	0.71
77.	380.4529	272.7	19.6	0.23	0.16	0.92	0.65
78.	380.7696	272.6	19.6	0.20	0.17	0.77	0.64
79.	381.0862	272.6	19.7	0.20	0.16	0.75	0.61
80.	381.4029	272.5	19.7	0.21	0.17	0.76	0.61
81.	381.7196	272.3	19.7	0.20	0.15	0.75	0.56
82.	382.0362	272.3	19.7	0.21	0.14	0.76	0.51
83.	382.3530	272.4	19.8	0.19	0.13	0.71	0.46
84.	382.6696	272.3	19.9	0.16	0.12	0.59	0.44
85.	382.9863	272.3	20.0	0.15	0.09	0.58	0.36
86.	383.3030	272.3	20.0	0.15	0.10	0.59	0.37
87.	383.6196	272.3	20.0	0.15	0.10	0.58	0.37
88.	383.9363	272.4	20.0	0.15	0.10	0.55	0.37
89.	384.2530	272.4	20.0	0.15	0.10	0.56	0.39
90.	384.5696	272.4	19.9	0.16	0.11	0.57	0.41

Table 2 (continued)

ORB.	START TIME	RT. ASCEN.	DEC.	SIG. R.A.	SIG. DEC.	RMS R.A.	RMS DEC.
91.	384.8863	272.5	19.9	0.17	0.12	0.61	0.42
92.	385.2030	272.5	19.8	0.16	0.11	0.60	0.41
93.	385.5196	272.6	19.8	0.16	0.11	0.60	0.42
94.	385.8363	272.6	19.7	0.16	0.12	0.59	0.43
95.	386.1530	272.7	19.6	0.16	0.12	0.62	0.44
96.	386.4696	272.8	19.6	0.15	0.11	0.56	0.42
97.	386.7863	272.7	19.5	0.14	0.11	0.55	0.43
98.	387.1030	272.7	19.4	0.14	0.12	0.55	0.45
99.	387.4196	272.7	19.3	0.15	0.13	0.56	0.47
100.	387.7363	272.5	19.0	0.20	0.17	0.73	0.61
101.	388.0530	272.5	19.0	0.15	0.13	0.57	0.50
102.	388.3696	272.6	19.0	0.17	0.14	0.60	0.51
103.	388.6863	272.6	19.0	0.17	0.14	0.60	0.51
104.	389.0030	272.7	19.0	0.20	0.17	0.72	0.61
105.	389.3196	272.8	19.1	0.19	0.20	0.69	0.72
106.	389.6362	272.8	19.0	0.19	0.19	0.68	0.73
107.	389.9529	272.8	19.0	0.19	0.19	0.70	0.72
108.	390.2696	272.9	19.1	0.23	0.20	0.85	0.74
109.	390.5862	273.0	19.2	0.23	0.16	0.85	0.59
110.	390.9028	273.1	19.2	0.14	0.16	0.50	0.57
111.	391.2195	273.1	19.3	0.19	0.17	0.69	0.58
112.	391.5361	273.1	19.2	0.23	0.20	0.85	0.73
113.	391.8528	273.0	19.1	0.19	0.16	0.65	0.54
114.	392.1694	272.9	19.1	0.18	0.15	0.63	0.54
115.	392.4861	273.0	19.1	0.14	0.12	0.48	0.43
116.	392.8028	272.9	19.1	0.15	0.14	0.49	0.45
117.	393.1194	272.8	19.0	0.13	0.13	0.49	0.48
118.	393.4360	272.8	19.0	0.15	0.17	0.55	0.62
119.	393.7526	272.6	18.8	0.13	0.13	0.50	0.49
120.	394.0693	272.5	18.8	0.13	0.14	0.50	0.54

Table 2 (continued)

ORB.	START TIME	RT. ASCEN.	DEC.	SIG. R.A.	SIG. DEC.	RMS R.A.	RMS DEC.
121.	394.3859	272.5	18.7	0.14	0.15	0.52	0.55
122.	394.7026	272.4	18.7	0.14	0.16	0.48	0.56
123.	395.0192	272.5	18.8	0.14	0.17	0.50	0.59
124.	395.3358	272.5	18.8	0.14	0.17	0.47	0.60
125.	395.6525	272.5	18.8	0.14	0.17	0.50	0.61
126.	395.9691	272.5	18.9	0.13	0.17	0.50	0.62
127.	396.2858	272.6	19.0	0.13	0.17	0.49	0.62
128.	396.6024	272.6	19.0	0.13	0.16	0.50	0.62
129.	396.9190	272.6	19.0	0.13	0.17	0.50	0.63
130.	397.2357	272.7	19.1	0.14	0.18	0.49	0.63
131.	397.5523	272.7	19.1	0.13	0.17	0.47	0.61
132.	397.8690	272.7	19.0	0.13	0.18	0.46	0.64
133.	398.1856	272.7	19.0	0.13	0.18	0.47	0.66
134.	398.5022	272.7	19.0	0.13	0.19	0.46	0.68
135.	398.8188	272.7	18.9	0.12	0.18	0.43	0.64
136.	399.1354	272.7	18.9	0.12	0.18	0.43	0.64
137.	399.4521	272.7	19.0	0.11	0.18	0.41	0.64
138.	399.7687	272.5	18.8	0.11	0.18	0.40	0.63
139.	400.0853	272.5	18.8	0.11	0.18	0.40	0.64
140.	400.4019	272.6	18.9	0.10	0.18	0.37	0.64
141.	400.7185	272.5	18.8	0.10	0.17	0.35	0.63
142.	401.0352	272.4	18.8	0.09	0.17	0.34	0.62
143.	401.3518	272.4	18.8	0.09	0.17	0.34	0.62
144.	401.6684	272.3	18.7	0.09	0.17	0.34	0.64
145.	401.9851	272.3	18.7	0.10	0.17	0.38	0.65
146.	402.3017	272.3	18.6	0.11	0.18	0.40	0.68
147.	402.6183	272.4	18.7	0.11	0.18	0.40	0.65
148.	402.9349	272.3	18.5	0.11	0.18	0.40	0.64
149.	403.2515	272.4	18.5	0.11	0.19	0.39	0.65
150.	403.5681	272.4	18.4	0.13	0.21	0.40	0.66

Table 2 (continued)

ORB.	START TIME	RT. ASCEN.	DEC.	SIG. R.A.	SIG. DEC.	RMS R.A.	RMS DEC.
151.	403.8848	272.3	18.1	0.13	0.21	0.42	0.71
152.	404.2014	272.2	17.9	0.13	0.22	0.43	0.70
153.	404.5180	272.2	17.8	0.14	0.23	0.47	0.74
154.	404.8346	272.2	17.7	0.15	0.24	0.48	0.76
155.	405.1512	272.2	17.5	0.16	0.24	0.48	0.75
156.	405.4678	272.1	17.4	0.15	0.24	0.47	0.76
157.	405.7844	272.1	17.2	0.16	0.25	0.48	0.75
158.	406.1010	272.2	17.3	0.16	0.25	0.50	0.81
159.	406.4176	272.4	17.4	0.13	0.23	0.43	0.74
160.	406.7342	272.5	17.4	0.14	0.24	0.46	0.78
161.	407.0508	272.6	17.4	0.14	0.24	0.46	0.78
162.	407.3674	272.7	17.4	0.14	0.24	0.47	0.79
163.	407.6840	272.7	17.2	0.16	0.27	0.49	0.83
164.	408.0006	272.7	17.2	0.16	0.26	0.49	0.83
165.	408.3171	272.7	17.2	0.15	0.25	0.48	0.82
166.	408.6337	272.7	17.0	0.14	0.25	0.47	0.82
167.	408.9503	272.7	17.0	0.14	0.25	0.46	0.83
168.	409.2669	272.8	17.0	0.14	0.25	0.46	0.84
169.	409.5835	272.7	16.9	0.12	0.23	0.42	0.81
170.	409.9001	272.8	16.9	0.12	0.23	0.44	0.86
171.	410.2167	272.8	17.0	0.13	0.25	0.46	0.88
172.	410.5333	272.9	16.9	0.13	0.25	0.46	0.88
173.	410.8500	272.8	16.8	0.12	0.22	0.45	0.86
174.	411.1664	272.9	16.8	0.12	0.24	0.46	0.89
175.	411.4830	272.9	16.7	0.12	0.24	0.42	0.87
176.	411.7996	272.9	16.6	0.12	0.25	0.42	0.87
177.	412.1162	272.9	16.5	0.13	0.25	0.42	0.87
178.	412.4327	272.9	16.5	0.12	0.25	0.41	0.86
179.	412.7493	272.9	16.5	0.12	0.25	0.41	0.87
180.	413.0659	272.9	16.6	0.11	0.24	0.40	0.86

Table 2 (continued)

ORB.	START TIME	RT. ASCEN.	DEC.	SIG. R.A.	SIG. DEC.	RMS R.A.	RMS DEC.
181.	413.3824	273.0	16.7	0.11	0.22	0.38	0.80
182.	413.6990	273.0	16.7	0.10	0.22	0.37	0.80
183.	414.0156	273.1	16.7	0.10	0.21	0.37	0.80
184.	414.3321	273.1	16.8	0.10	0.22	0.38	0.83
185.	414.6487	273.2	16.8	0.09	0.20	0.33	0.74
186.	414.9653	273.2	16.9	0.09	0.20	0.32	0.73
187.	415.2819	273.2	16.8	0.09	0.19	0.33	0.72
188.	415.5985	273.1	16.6	0.09	0.20	0.32	0.72
189.	415.9150	273.1	16.5	0.09	0.20	0.33	0.75
190.	416.2316	273.2	16.6	0.10	0.22	0.34	0.75
191.	416.5481	273.0	16.2	0.10	0.22	0.34	0.76
192.	416.8646	273.1	16.2	0.10	0.22	0.36	0.80
193.	417.1812	273.1	16.1	0.10	0.22	0.36	0.80
194.	417.4978	273.0	16.0	0.09	0.20	0.34	0.76
195.	417.8143	273.0	16.0	0.09	0.20	0.34	0.78
196.	418.1309	272.9	15.9	0.09	0.20	0.35	0.79
197.	418.4475	272.9	15.9	0.09	0.21	0.36	0.81
198.	418.7640	272.9	16.0	0.09	0.21	0.37	0.82
199.	419.0806	272.9	16.1	0.09	0.20	0.36	0.83
200.	419.3971	272.9	16.2	0.10	0.22	0.38	0.85
201.	419.7137	272.8	16.2	0.10	0.23	0.38	0.87
202.	420.0302	272.8	16.2	0.10	0.23	0.38	0.88
203.	420.3468	272.7	16.3	0.11	0.28	0.41	0.99
204.	420.6633	272.6	16.2	0.12	0.29	0.38	0.94
205.	420.9799	272.6	16.1	0.12	0.28	0.38	0.93
206.	421.2964	272.5	16.1	0.11	0.28	0.36	0.90
207.	421.6129	272.4	15.9	0.11	0.29	0.33	0.88
208.	421.9295	272.5	15.8	0.10	0.25	0.32	0.85
209.	422.2460	272.5	15.6	0.10	0.25	0.34	0.87
210.	422.5625	272.5	15.4	0.09	0.25	0.33	0.89

Table 2 (continued)

ORB.	START TIME	RT. ASCEN.	DEC.	SIG. R.A.	SIG. DEC.	RMS R.A.	RMS DEC.
211.	422.8791	272.5	15.4	0.09	0.25	0.31	0.91
212.	423.1956	272.5	15.4	0.08	0.25	0.30	0.90
213.	423.5121	272.6	15.4	0.08	0.26	0.28	0.89
214.	423.8286	272.7	15.4	0.09	0.26	0.29	0.89
215.	424.1452	272.7	15.4	0.08	0.25	0.28	0.87
216.	424.4617	272.7	15.3	0.08	0.26	0.28	0.86
217.	424.7782	272.7	15.3	0.08	0.27	0.28	0.88
218.	425.0948	272.7	15.2	0.07	0.21	0.23	0.72
219.	425.4113	272.7	15.2	0.06	0.22	0.21	0.76
220.	425.7278	272.8	15.1	0.06	0.21	0.21	0.75
221.	426.0443	272.8	15.1	0.06	0.23	0.21	0.81
222.	426.3608	272.8	15.1	0.06	0.23	0.21	0.81
223.	426.6773	272.8	14.7	0.07	0.26	0.24	0.89
224.	426.9938	272.9	14.7	0.07	0.28	0.25	0.96
225.	427.3102	272.9	14.7	0.08	0.27	0.27	0.94
226.	427.6268	273.0	14.7	0.08	0.26	0.27	0.89
227.	427.9433	273.0	14.7	0.08	0.27	0.26	0.90
228.	428.2598	273.1	14.6	0.08	0.27	0.26	0.90
229.	428.5763	273.1	14.2	0.06	0.25	0.24	0.92
230.	428.8927	273.2	14.0	0.06	0.23	0.24	0.86
231.	429.2093	273.2	13.9	0.06	0.24	0.25	0.92
232.	429.5258	273.3	13.7	0.06	0.24	0.25	0.92
233.	429.8423	273.5	13.6	0.07	0.23	0.26	0.90
234.	430.1587	273.6	13.5	0.06	0.22	0.25	0.88
235.	430.4752	273.7	13.4	0.07	0.25	0.27	0.95
236.	430.7917	273.8	13.2	0.08	0.26	0.29	0.96
237.	431.1082	273.9	13.3	0.08	0.27	0.29	1.02
238.	431.4247	274.0	13.5	0.08	0.27	0.28	0.96
239.	431.7411	274.1	13.4	0.07	0.23	0.26	0.90
240.	432.0576	274.2	13.5	0.06	0.22	0.23	0.87

Table 2 (continued)

ORB.	START TIME	RT. ASCEN.	DEC.	SIG. R.A.	SIG. DEC.	RMS R.A.	RMS DEC.
241.	432.3741	274.2	13.4	0.06	0.24	0.25	0.96
242.	432.6906	274.2	13.3	0.06	0.24	0.24	0.94
243.	433.0070	274.2	13.3	0.06	0.23	0.24	0.93
244.	433.3235	274.2	13.3	0.06	0.25	0.24	0.96
245.	433.6400	274.2	13.2	0.05	0.23	0.23	0.93
246.	433.9564	274.2	13.0	0.06	0.23	0.23	0.90
247.	434.2729	274.2	12.7	0.06	0.24	0.24	1.00
248.	434.5893	274.2	12.6	0.06	0.25	0.23	1.03
249.	434.9058	274.2	12.5	0.05	0.24	0.23	1.02
250.	435.2222	274.3	12.5	0.05	0.23	0.22	0.95
251.	435.5386	274.3	12.5	0.05	0.22	0.22	0.88
252.	435.8551	274.3	12.4	0.06	0.23	0.21	0.85
253.	436.1716	274.3	12.3	0.05	0.22	0.20	0.82
254.	436.4879	274.4	12.4	0.06	0.22	0.21	0.82
255.	436.8044	274.4	12.3	0.05	0.20	0.21	0.77
256.	437.1209	274.4	12.3	0.05	0.15	0.20	0.58
257.	437.4373	274.4	12.2	0.05	0.15	0.21	0.62
258.	437.7537	274.3	12.1	0.05	0.15	0.21	0.64
259.	438.0702	274.3	12.1	0.05	0.14	0.24	0.64
260.	438.3866	274.1	11.8	0.05	0.15	0.22	0.71
261.	438.7030	274.1	11.7	0.04	0.14	0.19	0.67
262.	439.0194	274.1	11.8	0.04	0.14	0.18	0.64
263.	439.3359	274.0	11.7	0.04	0.15	0.18	0.69
264.	439.6523	274.1	11.8	0.04	0.16	0.19	0.74
265.	439.9687	274.1	11.8	0.04	0.16	0.18	0.77
266.	440.2851	274.1	11.7	0.04	0.17	0.18	0.82
267.	440.6015	274.2	11.9	0.04	0.18	0.20	0.86
268.	440.9179	274.3	11.9	0.04	0.18	0.18	0.86
269.	441.2343	274.4	11.9	0.04	0.18	0.20	0.90
270.	441.5507	274.5	11.8	0.04	0.18	0.20	0.88

Table 2 (continued)

ORB.	START TIME	RT. ASCEN.	DEC.	SIG. R.A.	SIG. DEC.	RMS R.A.	RMS DEC.
271.	441.8671	274.6	11.7	0.04	0.18	0.19	0.88
272.	442.1836	274.7	11.5	0.04	0.18	0.21	0.91
273.	442.5000	274.8	11.4	0.04	0.18	0.20	0.90
274.	442.8163	274.9	11.2	0.04	0.18	0.20	0.88
275.	443.1327	275.0	11.1	0.04	0.19	0.20	0.94
276.	443.4492	275.0	10.8	0.04	0.19	0.20	0.95
277.	443.7656	275.1	10.7	0.04	0.18	0.20	0.91
278.	444.0820	275.2	10.6	0.04	0.18	0.21	0.90
279.	444.3984	275.3	10.5	0.04	0.19	0.20	0.95
280.	444.7148	275.4	10.3	0.04	0.18	0.20	0.92
281.	445.0311	275.5	10.5	0.04	0.16	0.20	0.81
282.	445.3475	275.5	10.3	0.04	0.16	0.20	0.81
283.	445.6639	275.7	10.3	0.04	0.16	0.19	0.80
284.	445.9802	275.7	10.3	0.03	0.15	0.18	0.78
285.	446.2966	275.8	10.1	0.03	0.17	0.17	0.88
286.	446.6130	275.9	10.1	0.03	0.18	0.18	0.90
287.	446.9294	276.0	10.1	0.03	0.17	0.16	0.88
288.	447.2457	276.0	9.8	0.03	0.19	0.16	0.97
289.	447.5621	276.1	9.8	0.03	0.19	0.17	0.98
290.	447.8785	276.2	9.8	0.03	0.19	0.17	0.94
291.	448.1948	276.3	9.7	0.03	0.19	0.17	0.94
292.	448.5112	276.3	9.7	0.03	0.20	0.17	1.00
293.	448.8275	276.4	9.6	0.03	0.19	0.16	0.98
294.	449.1438	276.5	9.4	0.03	0.19	0.16	0.97
295.	449.4602	276.5	9.2	0.03	0.20	0.16	1.01
296.	449.7766	276.6	9.0	0.03	0.19	0.15	0.98
297.	450.0929	276.6	9.0	0.03	0.19	0.17	1.00
298.	450.4093	276.6	8.9	0.03	0.20	0.16	1.01
299.	450.7256	276.7	8.8	0.03	0.19	0.16	0.97
300.	451.0419	276.7	8.7	0.03	0.18	0.17	0.89

Table 2 (continued)

ORB.	START TIME	RT. ASCEN.	DEC.	SIG. R.A.	SIG. DEC.	RMS R.A.	RMS DEC.
301.	451.3582	276.7	8.6	0.03	0.16	0.16	0.79
302.	451.6745	276.8	8.6	0.03	0.17	0.17	0.82
303.	451.9909	276.8	8.7	0.03	0.14	0.17	0.68
304.	452.3071	276.8	8.5	0.03	0.15	0.16	0.72
305.	452.6235	276.8	8.5	0.03	0.15	0.17	0.75
306.	452.9397	276.8	8.5	0.03	0.15	0.17	0.76
307.	453.2561	276.9	8.2	0.03	0.14	0.17	0.72
308.	453.5724	276.9	8.1	0.03	0.14	0.16	0.72
309.	453.8887	276.9	8.0	0.03	0.14	0.17	0.73
310.	454.2049	276.9	8.0	0.03	0.14	0.17	0.72
311.	454.5212	276.9	8.0	0.03	0.16	0.18	0.81
312.	454.8376	277.0	7.9	0.03	0.15	0.18	0.80
313.	455.1538	277.1	7.8	0.03	0.16	0.17	0.84
314.	455.4701	277.2	7.7	0.03	0.16	0.18	0.83
315.	455.7865	277.3	7.7	0.03	0.16	0.17	0.83
316.	456.1027	277.4	7.5	0.03	0.17	0.17	0.88
317.	456.4190	277.4	7.4	0.03	0.16	0.17	0.85
318.	456.7353	277.5	7.2	0.03	0.16	0.16	0.84
319.	457.0515	277.6	7.1	0.03	0.17	0.18	0.90
320.	457.3678	277.6	6.8	0.03	0.15	0.17	0.81
321.	457.6841	277.7	6.6	0.03	0.15	0.18	0.81
322.	458.0003	277.7	6.6	0.03	0.15	0.19	0.78
323.	458.3166	277.8	6.4	0.04	0.15	0.19	0.78
324.	458.6328	277.9	6.3	0.04	0.16	0.23	0.81
325.	458.9492	278.0	6.4	0.04	0.16	0.19	0.79
326.	459.2654	278.1	6.1	0.04	0.17	0.20	0.83
327.	459.5817	278.2	6.1	0.04	0.17	0.20	0.86
328.	459.8979	278.3	6.1	0.04	0.16	0.20	0.82
329.	460.2142	278.4	6.0	0.04	0.17	0.21	0.88
330.	460.5304	278.5	6.1	0.04	0.16	0.21	0.88

Table 2 (continued)

ORB.	START TIME	RT. ASCEN.	DEC.	SIG. R.A.	SIG. DEC.	RMS R.A.	RMS DEC.
331.	460.8467	278.6	6.0	0.04	0.15	0.20	0.83
332.	461.1629	278.7	5.8	0.04	0.15	0.20	0.88
333.	461.4792	278.8	5.8	0.03	0.17	0.20	1.00
334.	461.7953	278.9	5.7	0.03	0.16	0.19	0.91
335.	462.1116	279.0	5.6	0.03	0.17	0.20	0.97
336.	462.4278	279.1	5.5	0.03	0.17	0.19	0.98
337.	462.7441	279.2	5.4	0.03	0.17	0.18	0.99
338.	463.0603	279.3	5.3	0.03	0.18	0.18	1.00
339.	463.3765	279.4	5.1	0.03	0.18	0.17	0.98
340.	463.6927	279.5	5.0	0.03	0.17	0.18	0.97
341.	464.0089	279.6	5.0	0.03	0.16	0.17	0.91
342.	464.3251	279.7	4.9	0.03	0.17	0.18	0.96
343.	464.6413	279.8	4.7	0.03	0.17	0.19	0.96
344.	464.9575	280.0	4.6	0.03	0.16	0.18	0.94
345.	465.2737	280.1	4.4	0.03	0.16	0.19	0.92
346.	465.5899	280.3	4.4	0.03	0.16	0.19	0.92
347.	465.9061	280.4	4.5	0.03	0.15	0.20	0.86
348.	466.2223	280.6	4.4	0.04	0.15	0.20	0.87
349.	466.5385	280.7	4.4	0.03	0.16	0.20	0.89
350.	466.8546	280.8	4.4	0.04	0.14	0.20	0.79
351.	467.1708	281.0	4.3	0.04	0.14	0.21	0.79
352.	467.4870	281.1	4.3	0.04	0.15	0.22	0.83
353.	467.8032	281.3	4.3	0.04	0.14	0.20	0.80
354.	468.1194	281.4	4.2	0.04	0.15	0.20	0.82
355.	468.4356	281.6	4.2	0.03	0.15	0.19	0.84
356.	468.7517	281.8	4.1	0.03	0.15	0.19	0.83
357.	469.0678	281.9	3.9	0.03	0.14	0.17	0.76
358.	469.3840	282.1	3.8	0.03	0.15	0.18	0.81
359.	469.7002	282.3	3.7	0.03	0.14	0.18	0.80
360.	470.0163	282.4	3.6	0.03	0.15	0.17	0.84

Table 2 (continued)

ORB.	START TIME	RT. ASCEN.	DEC.	SIG. R.A.	SIG. DEC.	RMS R.A.	RMS DEC.
361.	470.3325	282.6	3.4	0.03	0.17	0.19	1.00
362.	470.6486	282.8	3.4	0.04	0.18	0.25	1.02
363.	470.9648	282.9	3.4	0.04	0.17	0.25	0.99
364.	471.2809	283.1	3.3	0.04	0.17	0.25	1.02
365.	471.5972	283.2	3.3	0.04	0.17	0.24	1.04
366.	471.9133	283.3	3.4	0.04	0.16	0.24	0.95
367.	472.2294	283.5	3.3	0.04	0.18	0.23	1.05
368.	472.5455	283.7	3.4	0.04	0.19	0.23	1.12
369.	472.8617	283.8	3.3	0.04	0.18	0.24	1.08
370.	473.1778	284.0	3.2	0.04	0.18	0.24	1.10
371.	473.4939	284.2	3.2	0.04	0.19	0.25	1.15
372.	473.8100	284.4	3.0	0.04	0.20	0.27	1.21
373.	474.1261	284.6	2.6	0.05	0.22	0.28	1.29
374.	474.4422	284.9	2.3	0.05	0.22	0.28	1.28
375.	474.7583	285.1	2.1	0.05	0.23	0.29	1.32
376.	475.0744	285.3	1.8	0.05	0.23	0.29	1.28
377.	475.3905	285.5	1.6	0.05	0.22	0.29	1.30
378.	475.7066	285.7	1.2	0.05	0.22	0.27	1.31
379.	476.0226	285.8	1.0	0.05	0.21	0.27	1.22
380.	476.3387	285.9	0.9	0.05	0.22	0.28	1.27
381.	476.6548	286.0	0.8	0.05	0.24	0.29	1.30
382.	476.9708	286.1	0.6	0.05	0.23	0.29	1.25
383.	477.2869	286.1	0.5	0.05	0.22	0.29	1.22
384.	477.6030	286.2	0.5	0.05	0.22	0.29	1.24
385.	477.9190	286.2	0.4	0.05	0.21	0.28	1.20
386.	478.2351	286.3	0.3	0.04	0.18	0.27	1.08
387.	478.5511	286.3	0.3	0.04	0.18	0.25	1.07
388.	478.8672	286.4	0.3	0.04	0.16	0.25	0.98
389.	479.1833	286.4	0.2	0.04	0.16	0.24	0.98
390.	479.4993	286.5	0.5	0.04	0.18	0.23	1.07

Table 2 (continued)

ORB.	START TIME	RT. ASCEN.	DEC.	SIG. R.A.	SIG. DEC.	RMS R.A.	RMS DEC.
391.	479.8153	286.6	0.3	0.04	0.16	0.22	1.01
392.	480.1313	286.7	0.1	0.03	0.16	0.22	1.00
393.	480.4474	286.8	0.3	0.04	0.17	0.23	1.06
394.	480.7634	286.9	0.3	0.04	0.16	0.25	1.06
395.	481.0794	287.1	0.1	0.04	0.16	0.26	1.01
396.	481.3954	287.2	0.3	0.04	0.17	0.26	1.09
397.	481.7115	287.4	0.2	0.04	0.17	0.29	1.09
398.	482.0274	287.6	-0.0	0.04	0.17	0.26	1.08
399.	482.3435	287.7	-0.1	0.04	0.17	0.29	1.13
400.	482.6594	287.9	-0.2	0.05	0.18	0.30	1.14
401.	482.9755	288.1	-0.4	0.05	0.19	0.30	1.16
402.	483.2915	288.3	-0.6	0.05	0.18	0.30	1.12
403.	483.6075	288.5	-0.8	0.05	0.19	0.31	1.15
404.	483.9235	288.7	-0.8	0.05	0.18	0.31	1.13
405.	484.2394	288.9	-1.0	0.05	0.16	0.31	0.96
406.	484.5555	289.0	-1.1	0.06	0.19	0.33	1.13
407.	484.8715	289.2	-1.0	0.06	0.20	0.34	1.12
408.	485.1874	289.4	-1.1	0.06	0.20	0.34	1.09
409.	485.5034	289.5	-0.9	0.06	0.21	0.34	1.14
410.	485.8194	289.7	-0.8	0.06	0.22	0.33	1.15
411.	486.1354	289.8	-0.9	0.06	0.18	0.32	0.99
412.	486.4514	289.9	-0.6	0.06	0.20	0.32	1.15
413.	486.7674	290.1	-0.6	0.06	0.19	0.33	1.08
414.	487.0833	290.2	-0.8	0.05	0.17	0.31	1.04
415.	487.3993	290.4	-0.7	0.05	0.18	0.32	1.11
416.	487.7153	290.5	-0.8	0.05	0.17	0.32	1.10
417.	488.0312	290.7	-0.9	0.05	0.16	0.31	1.06
418.	488.3472	290.8	-0.9	0.05	0.16	0.31	1.09
419.	488.6632	291.0	-0.9	0.05	0.17	0.32	1.11
420.	488.9792	291.1	-1.0	0.05	0.17	0.30	1.10

Table 2 (continued)

ORB.	START TIME	RT. ASCEN.	DEC.	SIG. R.A.	SIG. DEC.	RMS R.A.	RMS DEC.
421.	489.2951	291.3	-1.0	0.05	0.17	0.31	1.13
422.	489.6110	291.5	-1.1	0.05	0.17	0.31	1.12
423.	489.9270	291.6	-1.2	0.05	0.18	0.30	1.13
424.	490.2430	291.8	-1.3	0.05	0.17	0.29	1.09
425.	490.5589	292.0	-1.3	0.05	0.17	0.30	1.10
426.	490.8749	292.2	-1.4	0.05	0.17	0.35	1.09
427.	491.1908	292.4	-1.7	0.05	0.14	0.30	0.95
428.	491.5067	292.6	-1.6	0.05	0.16	0.34	1.09
429.	491.8226	292.8	-1.7	0.04	0.16	0.31	1.10
430.	492.1385	293.0	-1.9	0.05	0.15	0.32	1.07
431.	492.4545	293.1	-1.7	0.04	0.16	0.31	1.11
432.	492.7704	293.3	-1.7	0.05	0.17	0.34	1.19
433.	493.0863	293.4	-1.8	0.05	0.17	0.34	1.18
434.	493.4022	293.5	-1.6	0.05	0.17	0.33	1.24
435.	493.7181	293.6	-1.5	0.05	0.16	0.34	1.17
436.	494.0340	293.8	-1.8	0.04	0.15	0.31	1.10
437.	494.3499	293.9	-1.6	0.04	0.17	0.32	1.21
438.	494.6658	294.1	-1.6	0.05	0.17	0.34	1.19
439.	494.9817	294.2	-1.8	0.05	0.17	0.35	1.22
440.	495.2976	294.4	-2.0	0.05	0.17	0.34	1.21
441.	495.6135	294.6	-2.1	0.05	0.18	0.33	1.23
442.	495.9294	294.8	-2.2	0.05	0.18	0.33	1.26
443.	496.2453	294.9	-2.4	0.05	0.17	0.32	1.17
444.	496.5612	295.1	-2.4	0.05	0.17	0.35	1.20
445.	496.8771	295.2	-2.4	0.05	0.16	0.35	1.14
446.	497.1929	295.4	-2.5	0.05	0.16	0.35	1.10
447.	497.5088	295.5	-2.5	0.05	0.16	0.34	1.08
448.	497.8246	295.7	-2.5	0.05	0.15	0.34	1.04
449.	498.1406	295.8	-2.7	0.05	0.14	0.32	0.98
450.	498.4564	295.9	-2.5	0.05	0.15	0.33	1.02

Table 2 (continued)

ORB.	START TIME	RT. ASCEN.	DEC.	SIG. R.A.	SIG. DEC.	RMS R.A.	RMS DEC.
451.	498.7722	296.0	-2.4	0.05	0.14	0.33	0.99
452.	499.0881	296.2	-2.5	0.05	0.13	0.33	0.93
453.	499.4040	296.3	-2.4	0.05	0.14	0.35	1.04
454.	499.7198	296.5	-2.4	0.05	0.14	0.35	1.07
455.	500.0357	296.7	-2.5	0.05	0.13	0.34	1.00
456.	500.3515	296.9	-2.4	0.05	0.14	0.34	1.03
457.	500.6674	297.0	-2.3	0.05	0.14	0.34	1.01
458.	500.9832	297.2	-2.3	0.04	0.13	0.34	1.00
459.	501.2990	297.4	-2.3	0.05	0.14	0.34	1.03
460.	501.6149	297.7	-2.3	0.05	0.14	0.34	1.03
461.	501.9308	298.0	-2.5	0.04	0.14	0.33	1.02
462.	502.2465	298.2	-2.5	0.05	0.14	0.35	1.06
463.	502.5624	298.5	-2.5	0.05	0.15	0.38	1.11
464.	502.8782	298.7	-2.6	0.05	0.15	0.38	1.11
465.	503.1940	298.9	-2.7	0.05	0.15	0.39	1.08
466.	503.5098	299.2	-2.7	0.05	0.15	0.40	1.12
467.	503.8256	299.4	-2.7	0.05	0.16	0.38	1.13
468.	504.1414	299.7	-2.9	0.05	0.14	0.34	1.01
469.	504.4572	299.9	-2.9	0.05	0.15	0.35	1.06
470.	504.7731	300.1	-2.9	0.05	0.15	0.34	1.04
471.	505.0888	300.3	-2.8	0.05	0.15	0.33	1.01
472.	505.4046	300.5	-2.6	0.05	0.15	0.37	1.05
473.	505.7203	300.7	-2.6	0.05	0.15	0.36	1.07
474.	506.0362	301.0	-2.5	0.05	0.14	0.35	1.00
475.	506.3519	301.2	-2.4	0.05	0.15	0.36	1.06
476.	506.6677	301.4	-2.3	0.05	0.14	0.34	1.01
477.	506.9835	301.7	-2.4	0.04	0.13	0.34	0.97
478.	507.2992	301.9	-2.4	0.04	0.13	0.32	0.94
479.	507.6150	302.1	-2.4	0.04	0.13	0.32	0.94
480.	507.9308	302.4	-2.5	0.04	0.13	0.33	0.98

Table 2 (continued)

ORB.	START TIME	RT. ASCEN.	DEC.	SIG. R.A.	SIG. DEC.	RMS R.A.	RMS DEC.
481.	508.2465	302.6	-2.5	0.05	0.13	0.34	0.96
482.	508.5622	302.8	-2.5	0.05	0.13	0.34	0.96
483.	508.8780	303.0	-2.6	0.05	0.14	0.34	1.02
484.	509.1937	303.3	-2.7	0.05	0.14	0.33	0.97
485.	509.5094	303.5	-2.5	0.05	0.15	0.35	1.01
486.	509.8252	303.7	-2.5	0.05	0.15	0.35	1.03
487.	510.1410	303.9	-2.6	0.05	0.14	0.35	1.01
488.	510.4567	304.1	-2.4	0.05	0.15	0.35	1.03
489.	510.7724	304.4	-2.4	0.05	0.14	0.35	1.01
490.	511.0881	304.6	-2.5	0.05	0.13	0.34	0.95
491.	511.4038	304.8	-2.4	0.05	0.13	0.35	0.99
492.	511.7195	305.0	-2.3	0.05	0.13	0.35	1.00
493.	512.0353	305.3	-2.3	0.05	0.13	0.35	0.99
494.	512.3510	305.5	-2.2	0.05	0.13	0.36	1.00
495.	512.6667	305.7	-2.1	0.05	0.13	0.34	0.99
496.	512.9824	305.9	-2.1	0.04	0.13	0.33	0.97
497.	513.2981	306.2	-2.1	0.05	0.13	0.35	0.96
498.	513.6137	306.4	-2.0	0.05	0.13	0.37	0.95
499.	513.9294	306.6	-2.0	0.05	0.13	0.38	0.96
500.	514.2451	306.9	-2.0	0.05	0.13	0.39	0.93
501.	514.5608	307.2	-1.9	0.05	0.13	0.40	0.97
502.	514.8765	307.5	-2.0	0.06	0.13	0.44	0.98
503.	515.1921	307.7	-2.0	0.06	0.13	0.45	0.96
504.	515.5078	308.0	-2.0	0.07	0.14	0.47	0.98
505.	515.8235	308.3	-2.0	0.07	0.14	0.48	1.00
506.	516.1392	308.5	-2.0	0.07	0.13	0.52	0.97
507.	516.4549	308.8	-1.9	0.08	0.14	0.57	0.98
508.	516.7705	309.1	-1.9	0.09	0.15	0.62	0.99
509.	517.0861	309.3	-1.9	0.10	0.15	0.64	0.96
510.	517.4018	309.5	-1.8	0.12	0.15	0.73	0.94

Table 2 (continued)

ORB.	START TIME	RT. ASCEN.	DEC.	SIG. R.A.	SIG. DEC.	RMS R.A.	RMS DEC.
511.	517.7174	309.7	-1.8	0.14	0.16	0.80	0.95
512.	518.0331	310.0	-1.8	0.14	0.16	0.84	0.98
513.	518.3487	310.1	-1.7	0.15	0.15	0.90	0.93
514.	518.6644	310.3	-1.7	0.16	0.16	1.01	1.01
515.	518.9801	310.6	-1.8	0.16	0.16	1.06	1.04
516.	519.2957	310.8	-1.7	0.16	0.13	1.10	0.88
517.	519.6113	311.1	-1.6	0.16	0.15	1.13	1.05
518.	519.9269	311.4	-1.7	0.17	0.17	1.17	1.14
519.	520.2426	312.0	-1.6	0.23	0.17	1.58	1.14
520.	520.5582	312.2	-1.7	0.23	0.17	1.68	1.22
521.	520.8738	312.5	-1.7	0.24	0.18	1.74	1.24
522.	521.1894	312.8	-1.7	0.25	0.18	1.85	1.25
523.	521.5050	313.2	-1.7	0.25	0.20	1.81	1.40
524.	521.8206	313.0	-1.7	0.22	0.21	1.52	1.48
525.	522.1362	313.3	-1.6	0.22	0.22	1.57	1.52
526.	522.4518	313.4	-1.5	0.24	0.23	1.66	1.59
527.	522.7674	313.7	-1.2	0.28	0.30	1.93	2.06
528.	523.0830	313.9	-1.5	0.28	0.23	1.92	1.56
529.	523.3986	314.0	-1.4	0.27	0.23	1.80	1.57
530.	523.7142	314.2	-1.3	0.26	0.23	1.74	1.56
531.	524.0297	314.4	-0.9	0.25	0.28	1.73	2.01
532.	524.3454	314.7	-1.1	0.25	0.24	1.70	1.66
533.	524.6609	314.9	-1.0	0.25	0.23	1.68	1.58

PRECEDING PAGE BLANK NOT FILMED.

APPENDIX C

FIGURES

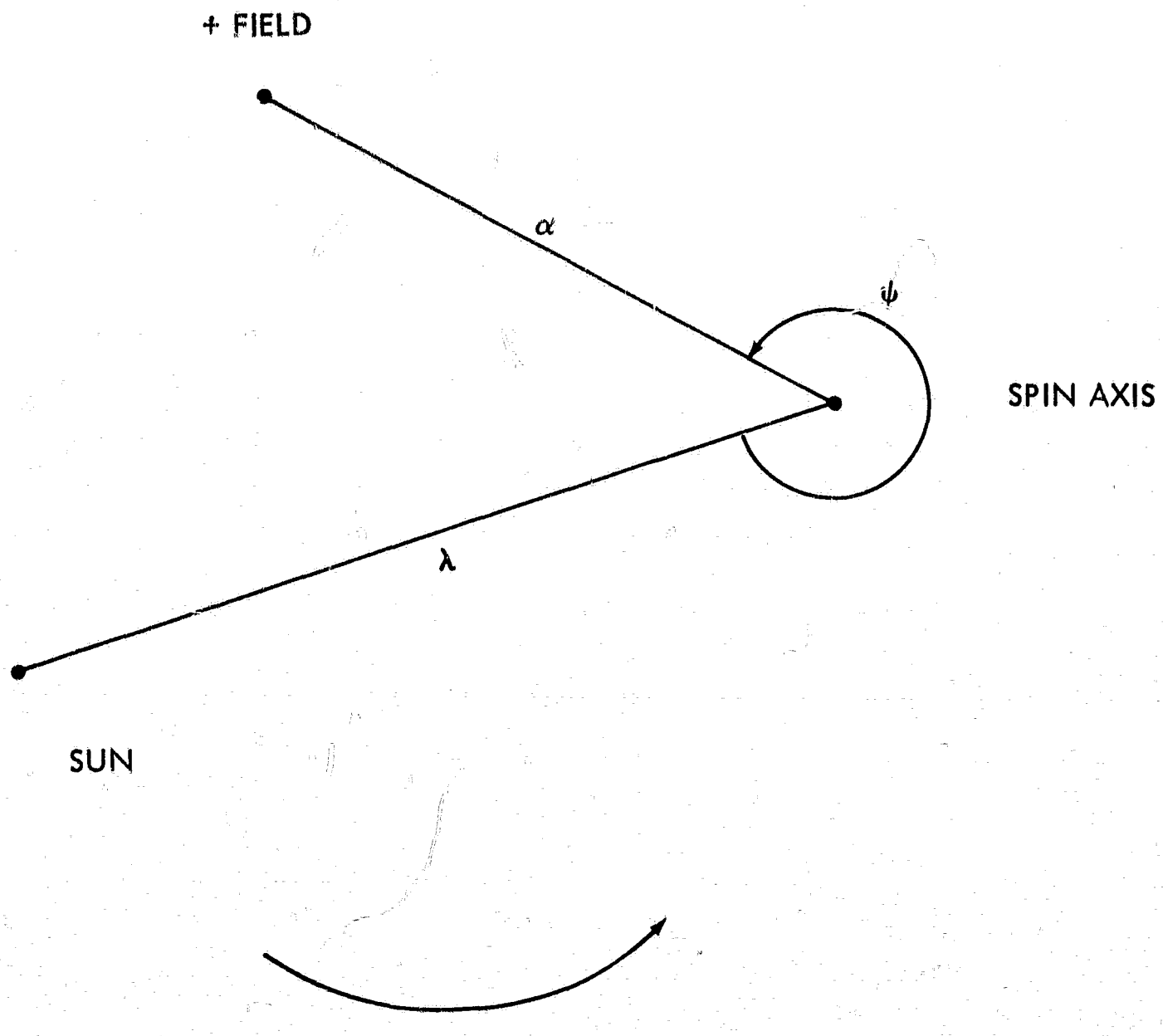

Figure 1. λ, α, ψ, Plotted as on the Celestial Sphere

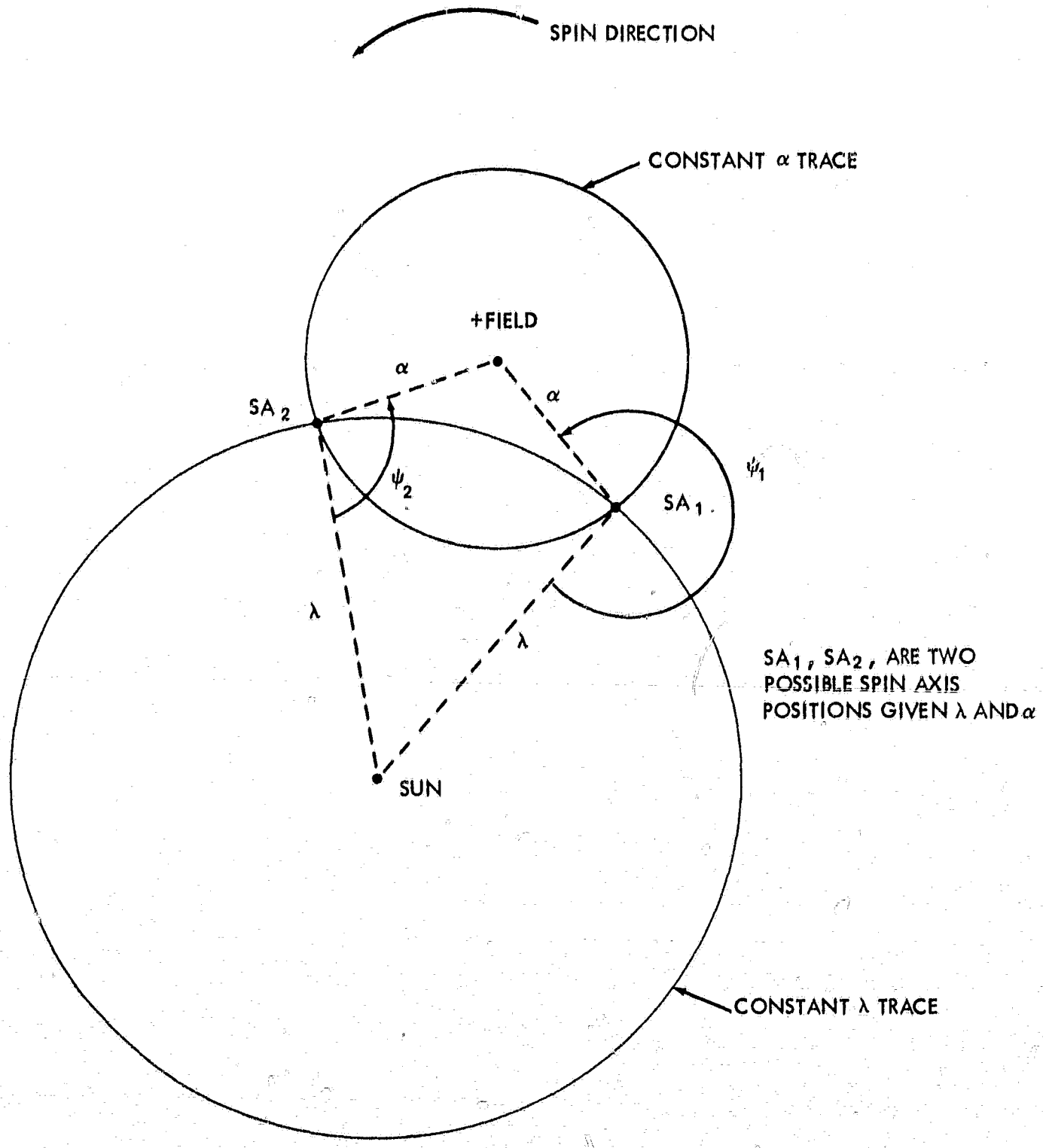

Figure 2. Spin Axis Determination–Plotted as on the Celestial Sphere

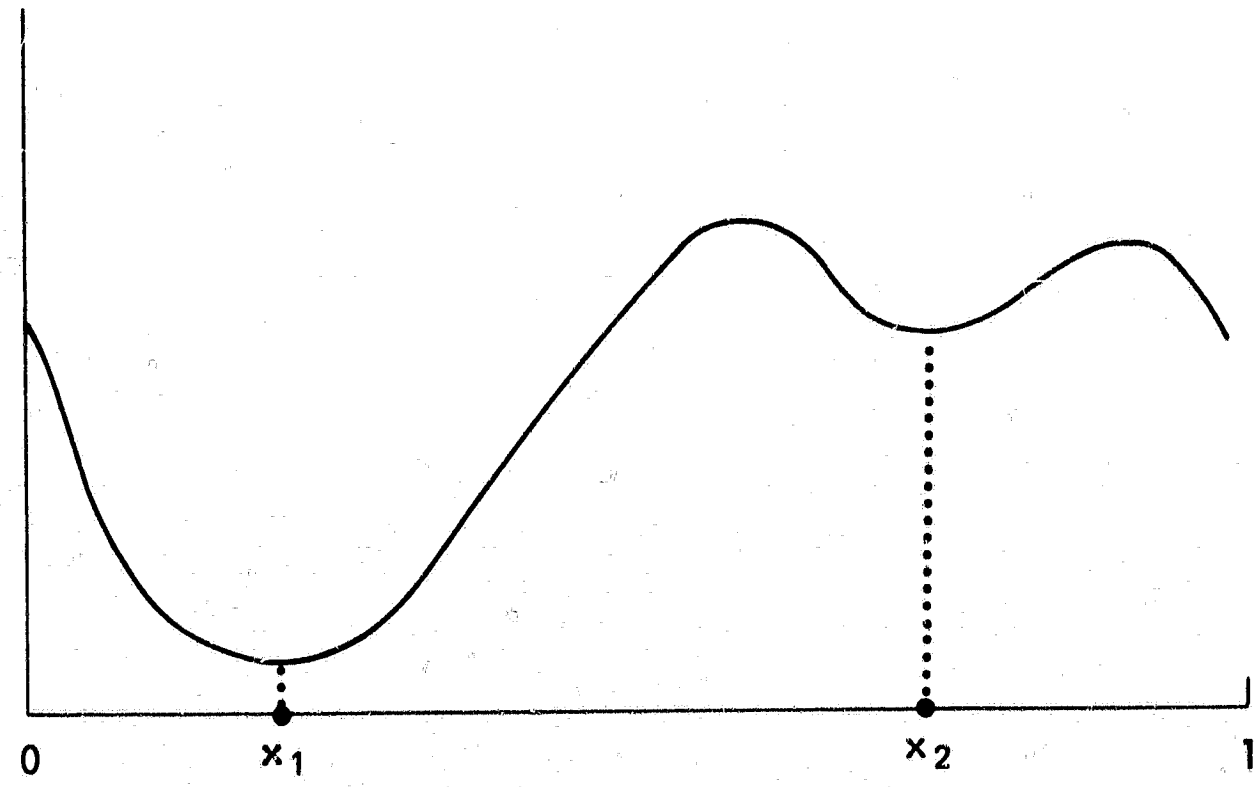

Figure 3. Relationship of ψ to the I&E Detector Output Curve

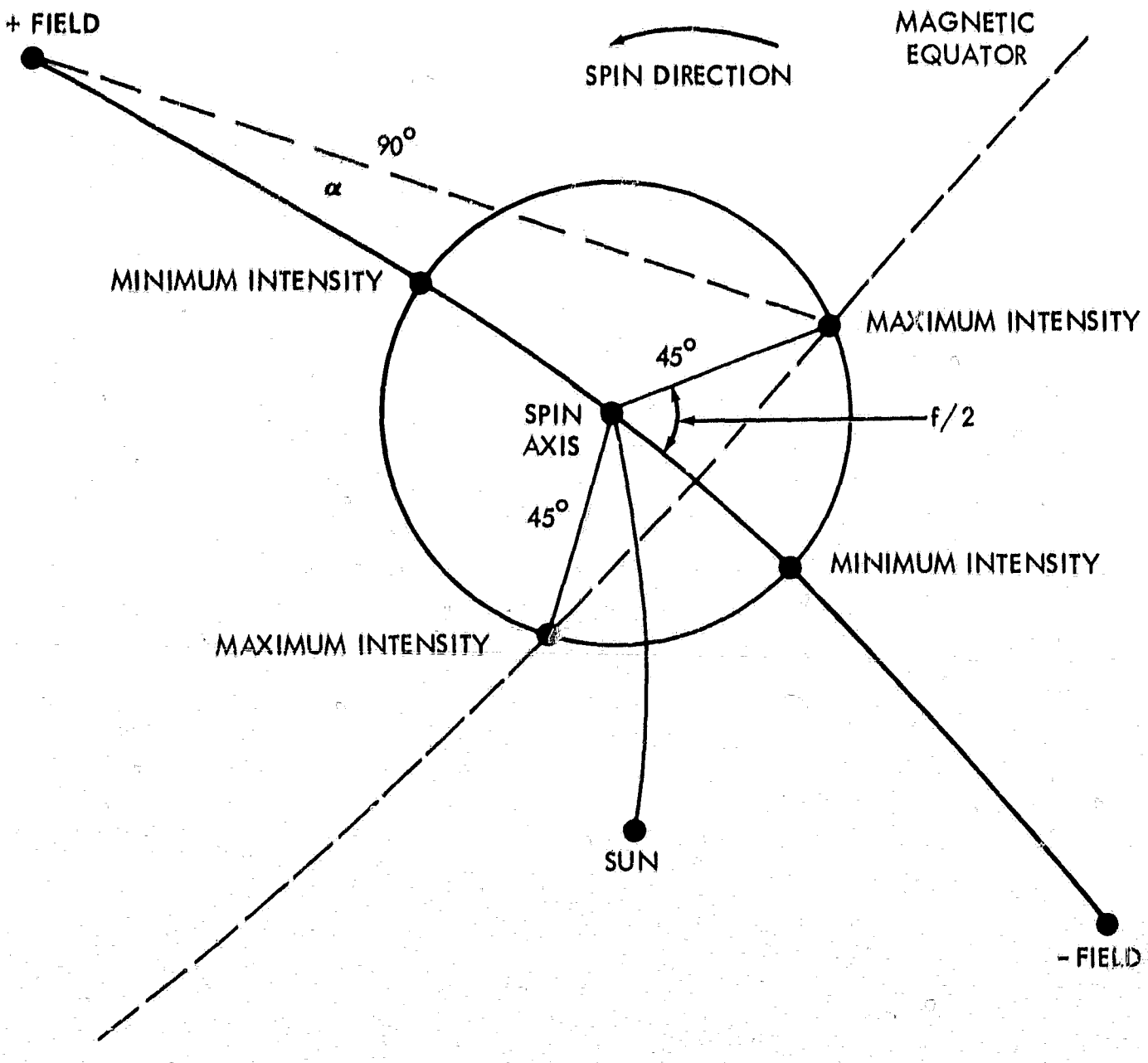

Figure 4. α as a Function of the Fraction of a Roll Between Maxima as Plotted on the Celestial Sphere

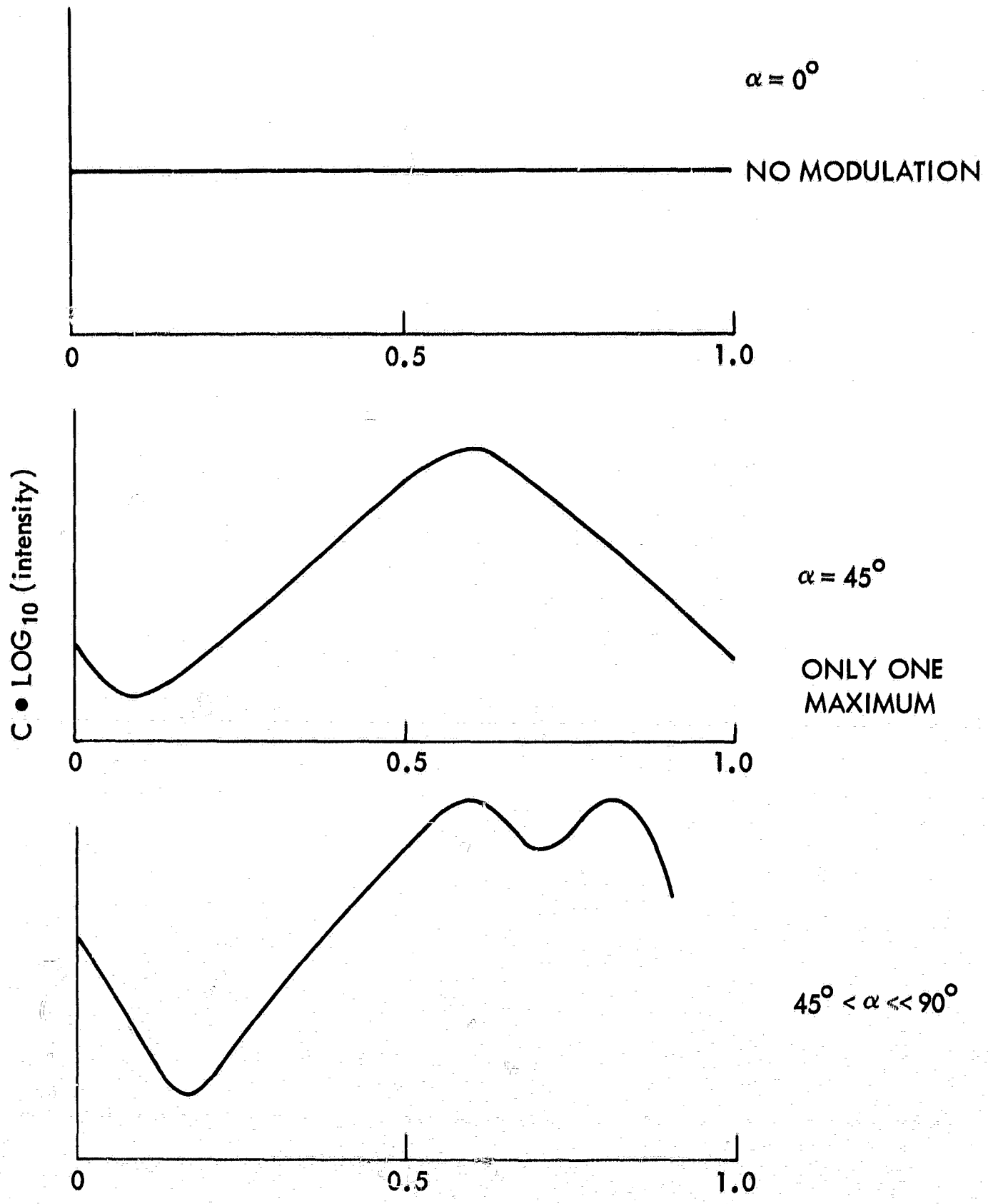

Figure 5. I&E Roll Modulation Curves for Values of α up to 90°

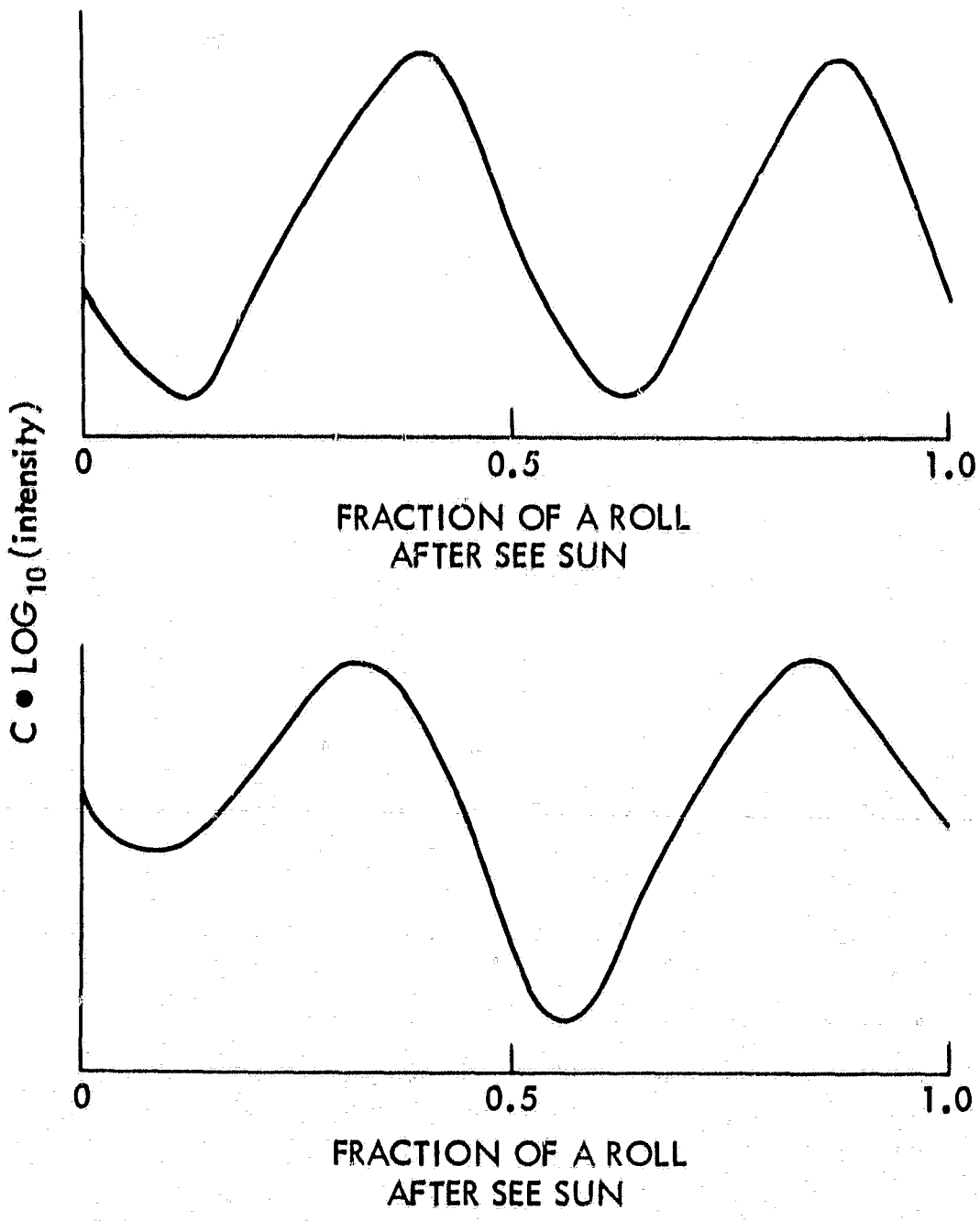

Figure 6. I&E Roll Modulation Curves for Values of α from 90° to 135°

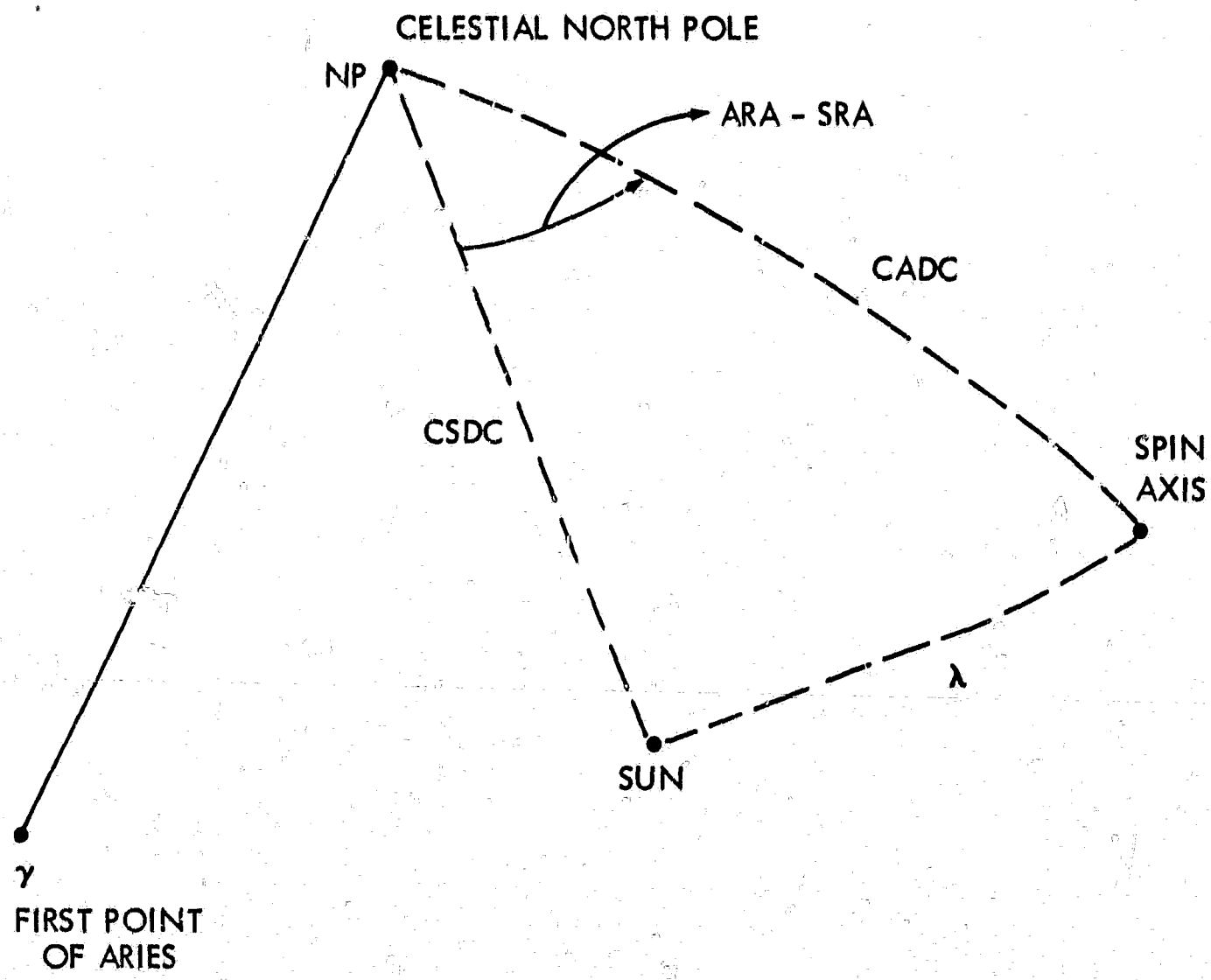

Figure 7. Calculated Values for λ

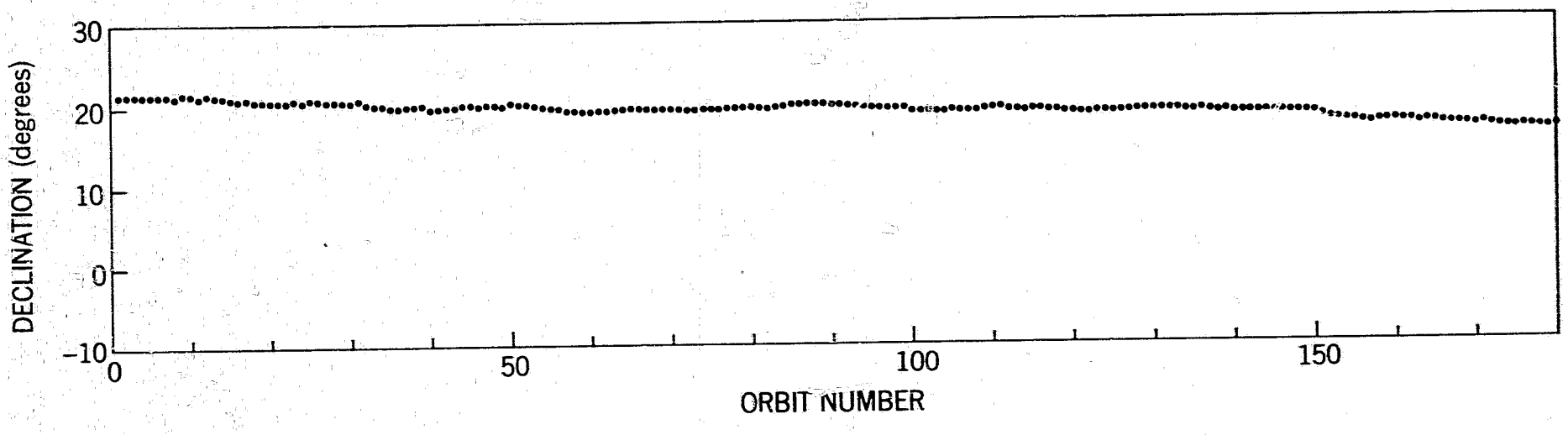

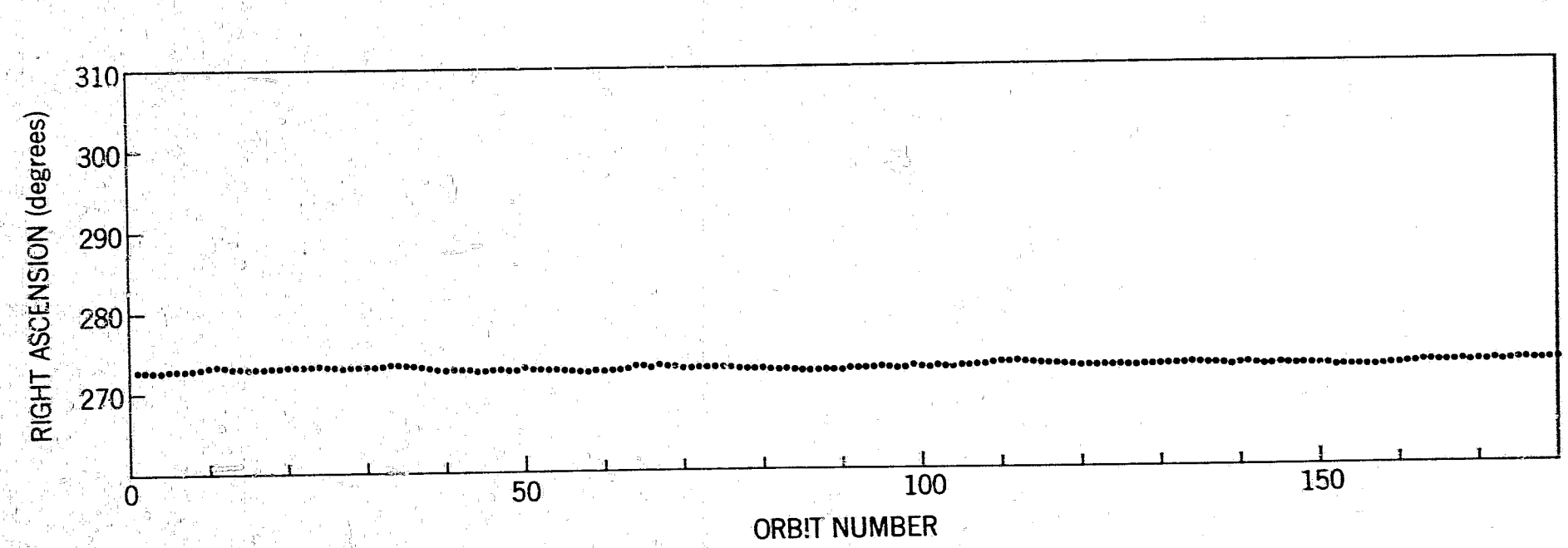

Figure 8a. Explorer XXVI Spin Axis Coordinates

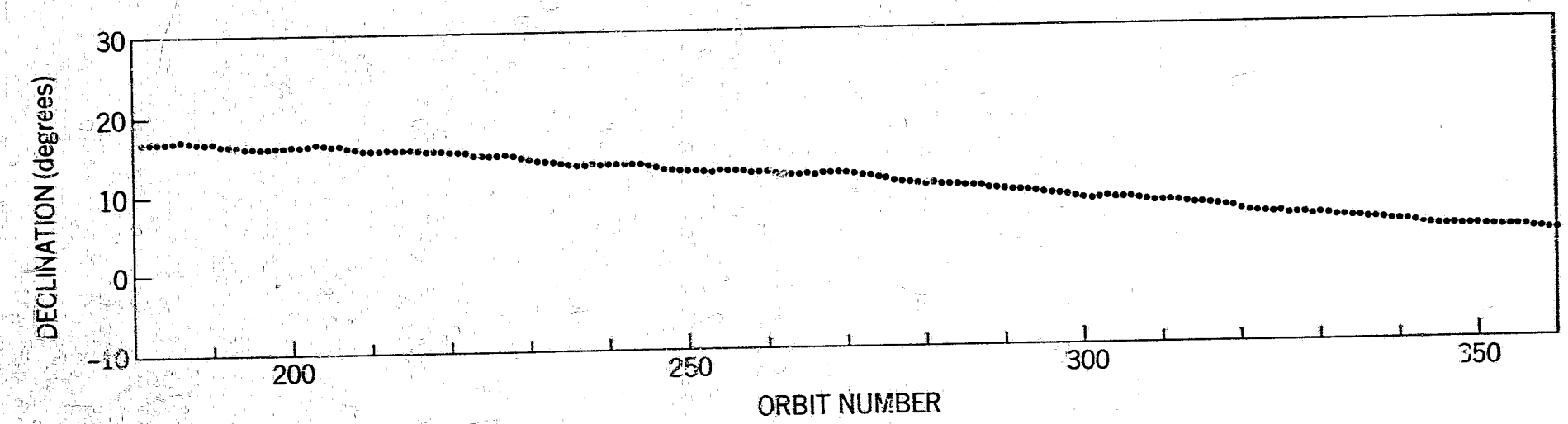

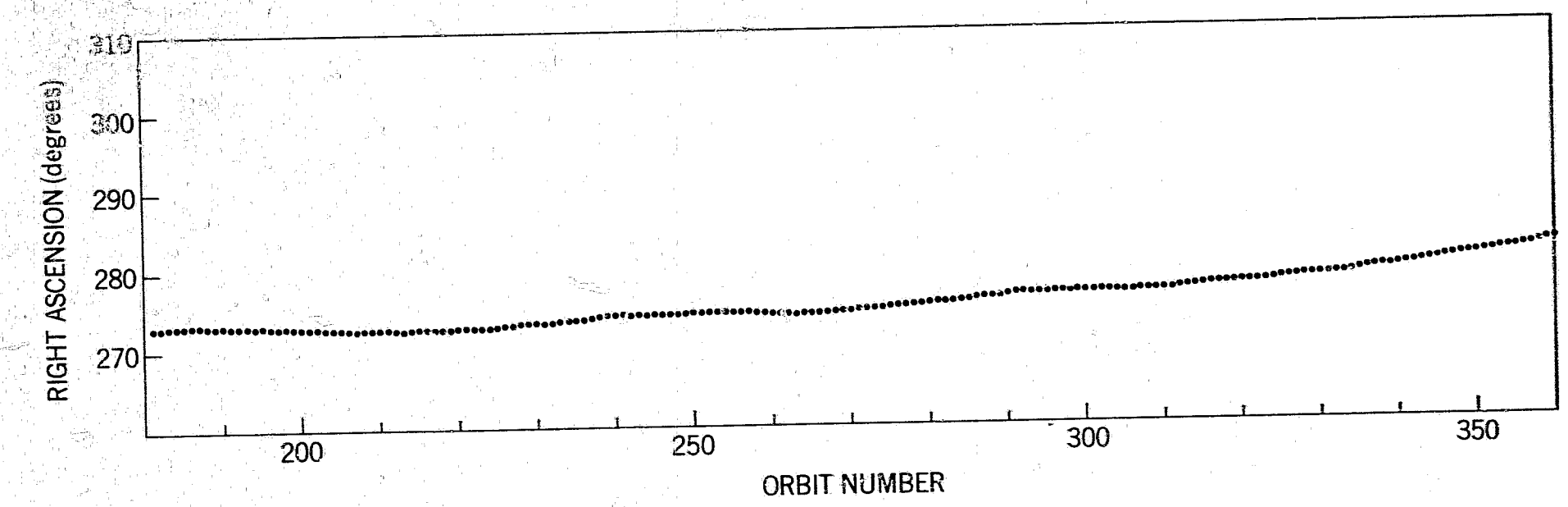

Figure 8b. Explorer XXVI Spin Axis Coordinates

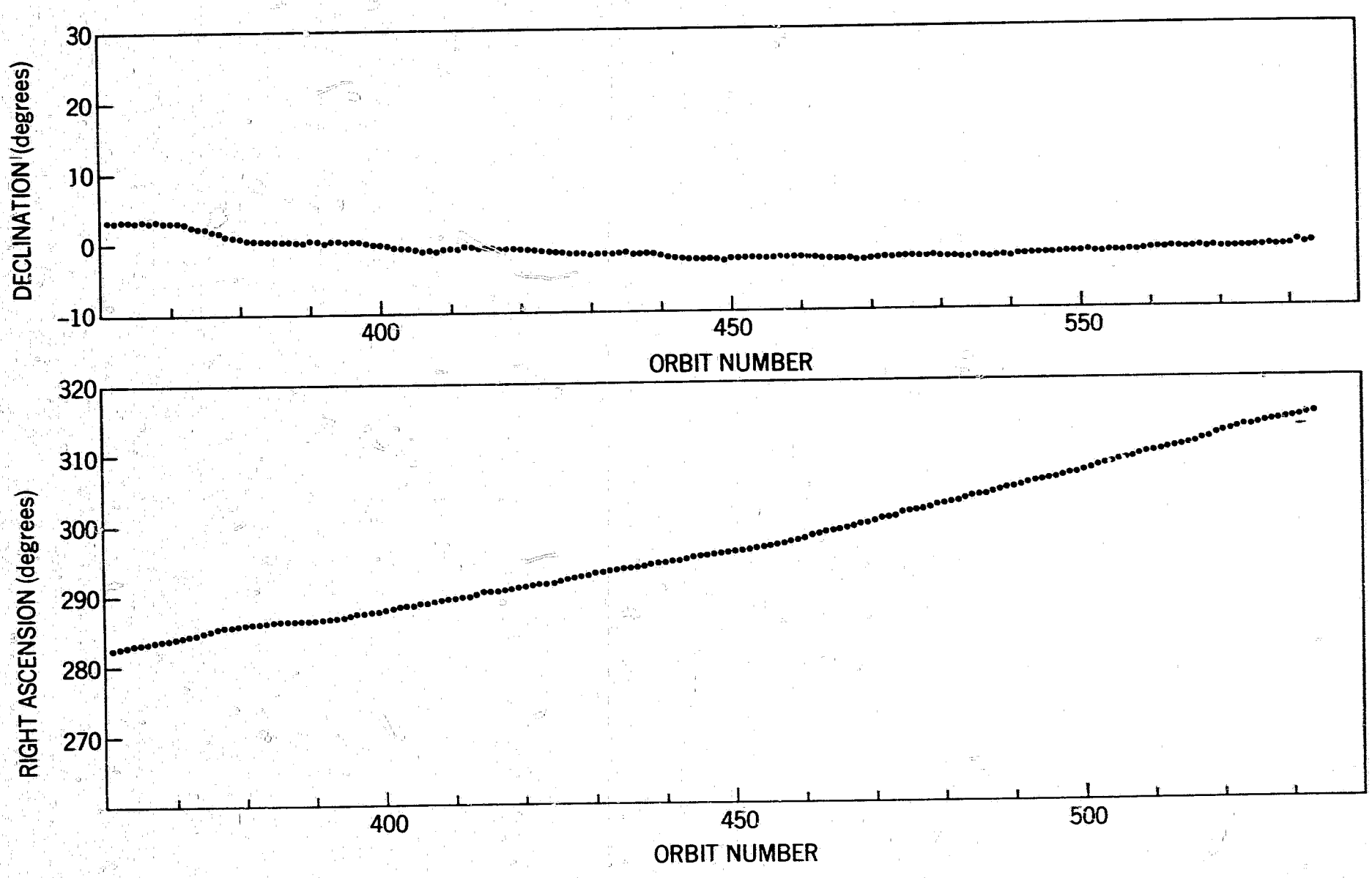

Figure 8c. Explorer XXVI Spin Axis Coordinates